Department of Hydrology

Albert-Ludwigs-University Freiburg

Master Thesis

A new method for continuously measuring isotopic signatures of soil pore water in the field:

comparison with destructive sampling and applicability to address ecohydrological questions

*

Sinikka Jasmin Paulus

Master programme Hydrology, Albert-Ludwigs-University Freiburg

Advisor: Maren Dubbert PhD

Department of Ecosystem Physiology;
Albert-Ludwigs-University Freiburg

Co-advisor: Natalie Orlowski PhD

Department of Hydrology;
Albert-Ludwigs-University Freiburg

Contents

List of Figures

List of Tables

Acknowledgements

At this point I would like to express my sincere thanks to my first supervisor Dr. Maren Dubbert, who always helped me with food for thought, encouraging words and a lot of optimism. Thank you very much for letting me get so deeply involved in the field of ecosystem physiology and for trusting in me and my work. I am very grateful for Dr. Natalie Orlowski being my second supervisor and for sharing her wealth of experience and contributing valuable ideas to improve this thesis.

My special thanks go to Angelika Kübert for her close support throughout the work and for all the time it took to answer my infinite number of questions. Thanks also for your support in the field. I highly acknowledge Adrian Dahlmanns significant contribution to the creation of this work within the framework of his bachelor's thesis and his position as undergraduate research assistant. Thanks for the many drill cores you pulled out of the soil and the support at the cryogenic extraction facility. My parents and grandparents are also thanked for supporting me throughout my studies and giving me the opportunity to take so much time for my university education. Not to be forgotten, I would also like to thank all people involved in proofreading for their valuable critics. A special thanks goes to all my friends supporting me in general during the time of the creation of this thesis.

Abstract

Analysis of H and O stable isotope ratios (δ^2H and δ^{18}O values) have gained increasing importance in ecohydrological research. Since the development of Cavity Ring-Down Spectroscopy (CRDS), measurements are of high temporal resolution and good accuracy. However, sample collection still remains challenging and new methods are still being developed to exploit the full potential of this promising measuring technology. In this study, we investigated a laboratory-tested sampling technique that enables continuous *in situ* monitoring of the isotopic composition of soil pore water vapour. We present an *in situ* field application of this method in a labelling experiment in a temperate grassland. Parallel to the soil we measured *in situ* plant transpiration water isotope measurements of two grassland species. Additionally, we compared our observations with the isotopic signatures of destructive soil and leaf samples from which water was extracted by means of cryogenic vacuum extraction. Furthermore, results were used as input for a Bayesian multi-source mixing model (BIMM) to investigate which impact the choice of different methods - *in situ* or destructive - had on the simulation of root water uptake (RWU) depth.

The benchmarking of the different model inputs, i.e. *in situ* and destructive sampling, illustrates the usefulness of *in situ* non-destructive sampling to investigate spatiotemporal processes at the soil-vegetation-atmosphere interface. The possibility to measure repeatedly at identical locations and in daily resolution with high accuracy, allowed us to discern temporal dynamics of the water isotopic signature from lateral heterogeneity. The labelling approach facilitated spatio-temporal differenciation between different soil layers. Systematic offsets between results from *in situ* and destructive sampling provide further evidence for delayed exchange of isotopes between incoming and more tightly bound fractions of water in the soil matrix. The comparison of transpiration isotopic values revealed destructive sampling to be afflicted with higher scattering. This could be attributed to uncertainties of input-parameter estimates when deriving transpiration isotopic signatures from bulk leaf water. Our study contributes to recent development of more targeted sampling techniques in ecohydrological research. Furthermore, this investigation underlines the necessity to combine expert knowledge from several disciplines, such as soil, plant physiology and hydrology to enhance data reliability and advance RWU research.

Keywords: stable water isotope analysis, soil-vegetation-atmosphere interface, ecohydrology, labelling experiment, soil water extraction, mixing model, root water uptake

Zusammenfassung

Die stabilen Wasserisotope ^{18}O und ^{2}H sind von wachsender Bedeutung in der Erforschung ökohydrologischer Zusammenhänge. Sie ermöglichen es, Wasserflüsse zwischen unterschiedlichen Kompartimenten in Ökosystemen voneinander zu differenzieren und sie zu quantifizieren. Seit Entwicklung der Cavity Ring-Down Spektroskopie ist es möglich, Wasserisotope in der Gasphase präzise und mit hoher zeitlicher Auflösung zu messen. Die Technologie birgt somit erstmals das Potenzial, die Wasseraufnahme von Pflanzen direkt messbar zu machen. Damit kann sie einen wichtigen Beitrag zur Verbesserung unseres Prozessverständnisses auf unterschiedlichen zeitlichen und räumlichen Skalenebenen leisten. Dies ist insbesondere vor dem Hintergrund prognostizierter Veränderungen in der Niederschlagsmenge und -intensität durch den Klimawandel von Bedeutung, um die Auswirkungen auf Ökosysteme abzuschätzen und Anpassungsstrategien zur Erhöhung von ökosystemarer und landwirtschaftlicher Resilienz zu entwickeln. Die Probenahme stellt allerdings weiterhin eine Herausforderung dar und limitiert damit die Nutzung des vollen Potenzials der neuen Messtechnik.

Im Rahmen dieser Arbeit wurde ein Aufbau mit *in situ* Messsonden aus Polypropylenmembran zur Beprobung der Bodengasphase mit täglicher Auflösung unter Feldbedingungen über einen Zeitraum von 33 Tagen getestet. Mit Hilfe der Isotopensignatur des gasförmigen Porenwassers konnte die Signatur der residualen Flüssigphase bestimmt werden. Zusätzlich wurden regelmäßig stabile Isotope in der Transpiration von *Centaurea jacea* und *Arrhenaterum elatius in situ* auf Blattebene gemessen. Zum Vergleich wurden zeitlich parallel zum *in situ* Versuchsaufbau Bohrkerne gezogen und Blattbiomasse geerntet. Diese aus destruktiver Probenahme stammenden Proben wurden im Labor mittels kryogener Vakuumdestillation extrahiert und die Isotopensignatur des so erhaltenen Wassers analysiert.

Die experimentelle Feldarbeit wurde auf einem Grünlandstandort in Mitteleuropa durchgeführt. Die Bodenfeuchtekonditionen auf der Versuchsfläche wurden über Rainoutshelters manipuliert und zwei Starkregensimulationen mit isotopisch markiertem Wasser wurden aufgebracht. Ergebnisse der *in situ* und der destruktiven Messungen wurden in einem Bayesian multi-source mixing model (BIMM) verwendet, um die Effekte der unterschiedlichen Messmethoden auf die ökohydrologische Interpretation aufzuzeigen. Unsere Ergebnisse zeigen, dass die unter Laborbedingungen entwickelte *in situ* Methode unter den gegebenen Bedingungen konsistente Messungen im Feld ermöglichte. Die Präzision war ausreichend, um zeitliche und räumliche Dynamiken der Wasserflüsse voneinander zu differenzieren. In Kombination mit *in situ* Transpirationsmessungen konnten zeitlich konsistente Aufnahmemuster zweier Grünlandarten als Reaktion auf Starkniederschlagsereignisse nach Trockenheit modelliert werden. Systematische Unterschiede zwischen den Ergebnissen der angewendeten Methoden wurden sowohl für das Boden- als auch für das Pflanzenmaterial festgestellt.

Unser Versuchsaufbau ermöglicht einen Einblick auf die Auswirkungen von Starkregenereignissen nach Trockenphasen auf die Anpassungsstrategien zweier funktionell unterschiedlicher Grünlandarten. Des Weiteren sind die Ergebnisse ein zusätzlicher Hinweis darauf, dass kontinuierliche Messungen mit hoher zeitlicher Auflösung sowohl die Entwicklung besserer mechanistischer Modelle zur Simulation von Vegetations-Atmosphären Interaktion vorantreiben, als auch zur Auflösung der Debatte um mobile und immobile Bodenwasserkompartimente beitragen können.

1 Introduction

Global climate change projections predict significant changes in the rainfall distribution pattern and amount for Central Europe (Solomon et al. 2007). Since plant biomass is directly linked to water availability, changes in the water regime are expected to influence the productivity of many natural terrestrial ecosystems as well as agricultural areas (Dubbert et al. 2013, Dubbert, Piayda, Cuntz & Werner 2014). Due to their shallow root system, grassland ecosystems are often strongly dependent on soil water. Because they are usually not connected to groundwater, occasional rain events control the soil water regime in these environments.

However, soil water availability is highly variable in space and time, depending on precipitation input and soil attributes. Modelling moisture dynamics and plant responses requires knowledge of soil hydraulic properties as well as vegetation reaction and climatic conditions (Schymanski et al. 2008). There is a long tradition of estimating root water uptake (RWU) based on underground plant biomass but direct measurements are rare or absent (Kulmatiski & Beard 2013, Rothfuss & Javaux 2017). The reason is a lack of appropriate methodology (Volkmann et al. 2016).

Due to these knowledge gaps in the dynamics and mechanistic controls of RWU patterns, the soil environment is the weakest component of soil-vegetation-atmosphere transfer models (Schymanski et al. 2008). The development of more physically based modelling approaches to enhance estimation of climate impacts on soil and plants requires an improved understanding of temporal changes in water availability and root water uptake in the soil (Berry et al. 2018). The functional understanding of soil-vegetation feedbacks is therefore of major interest in the rapidly evolving field of ecohydrology.

Stable water isotopes are considered ideal water flow tracers and are utilized to improve knowledge about the estimation of soil evaporation rates, hydraulic redistribution in soils, percolation and groundwater recharge, as well as the separation of evaporation and transpiration (Sprenger et al. 2016). The share of heavy water isotopes (^{18}O, ^{2}H) in the water molecules, relative to the more abundant form (^{16}O, ^{1}H), and the relation between the two heavy water isotopes is altered during phase changes. Evaporation of water from a surface, for example, leads to an enrichment of residual water.

The developing natural differences in the isotopic composition between compartments of an ecosystem are used to distinguish and quantify storage and flux dynamics of water. Furthermore, oxygen and hydrogen stable isotope analysis in soil and in plants enables to trace water movement within the soil-plant-atmosphere continuum (Yakir & Sternberg 2000). Since plant water uptake is considered as a non-fractionating process (Ehleringer & Dawson 1992), the isotopic signature of xylem water reflects an integral measure of the soil water at water uptake depth of the roots (Evaristo et al. 2017). Within the last decade, a rising number of investigations used end-member mixing analysis, to statistically determine the contribution of different soil depths to the plant water isotopic signal (Rothfuss & Javaux 2017). As yet, plant and soil material is predominantly sampled destructively. Containing water is extracted in the laboratory by cryogenic vacuum distillation (Orlowski et al. 2013, Rothfuss & Javaux 2017). Because of the approach's destructive nature, the validity of temporal processes is limited. Berry et al. (2018) are addressing the methodological state of the art in stable isotope ecohydrology as "shotgun" or "snapshot methods", referring to the lack of continuous measurements. Moreover, these technical constraints also limited the development of more physically based root water uptake models (Rothfuss & Javaux 2017). Additionally, extraction methods are currently highly debated due to inaccurate results. These depend on soil texture

and laboratory extraction procedure (Orlowski et al. 2016, 2018). A recent study from Sprenger et al. (2018) is indicating, that different residence times of water at the pore scale affect isotopic signatures of the soil water. Hence, cryogenic extracted material might not be representative for processes at different temporal scales (Sprenger et al. 2018, Berry et al. 2018). Several authors have addressed the lack of methodology in stable isotope research and called for an improvement of spatial and temporal resolution of soil pore water, vapour fluxes and plant transpiration measurements (Volkmann et al. 2016, Rothfuss & Javaux 2017, Berry et al. 2018, Dubbert & Werner 2018).

With the development of new methods in water isotope measurement technology, new opportunities arise to measure water stable isotopes *in situ*. Techniques based on laser spectroscopy have been successfully used in recent years to measure water vapour isotopic composition at high precision and high frequency. Several research groups have developed and tested microporous sampling probes to sample soil water isotope composition *in situ* in a non-destructive manner (Rothfuss et al. 2013, Volkmann & Weiler 2014, Gaj et al. 2016). So far, these methods have been mainly applied for continuous measurements under controlled laboratory conditions (Rothfuss et al. 2015, Quade et al. 2018) or on short timescales in the field (maximum 11 consecutive days) (Volkmann et al. 2016, Gaj et al. 2016). The only longterm experiment under field conditions was conducted by Oerter et al. (2017), who successfully monitored soil water stable isotopes over several months in an urban area. Despite few applications, the potential of *in situ* longterm monitoring experiments has been addressed by numerous studies and reviews within the field of ecohydrology (Sprenger et al. 2015, Stumpp et al. 2018, Penna et al. 2018, Berry et al. 2018).
Concurrently, continuous measurements of the isotopic composition in transpired water were tested on leaf and plant community scale. The methods found increasing application (Wang et al. 2012, Dubbert et al. 2013, 2017) and allowed the improvement of leaf morphology based transpiration models due to the possibility to monitor living plant organism (Farquhar & Cernusak 2005, Dubbert et al. 2017). Still, these models require a number of parameters that are labourious to obtain or not straightforward to measure (Farquhar & Cernusak 2005).

The combination of *in situ* soil water stable isotope measurements and *in situ* plant transpiration measurements offers new possibilities to disentangle ecological soil vegetation feedbacks (Volkmann & Weiler 2014, Rothfuss et al. 2015, Sprenger et al. 2016). Volkmann et al. (2016), were able to show with continuous *in situ* measurements how different tree species under drought varied in their reaction towards an artificial precipitation pulse. Their results showed that the response was visible within one to four hours after the rain event occurred and that the reactions were species-specific. In order to evaluate the relevance of the observed pattern for different vegetation forms and on longer timescales, more experiments of this type are needed. For example, seasonal variation of RWU might play a role due to different requirements of growth in plants (Dubbert, Piayda, Cuntz, Correia, Costa e Silva, Pereira & Werner 2014). The mechanism of niche complementarity in plant water uptake in systems of high biodiversity are also still not clearly understood (Werner et al. 2012, Bachmann et al. 2015, Rothfuss & Javaux 2017). Kulmatiski & Beard (2013) suggested that the effect might be no fixed mechanism but rather a plant community reaction on a short spatial and temporal scale. In particular, high uncertainties exist concerning the reaction of ecosystems in dry conditions, when plants need to optimize cost and benefit between transpiration and biomass production (Schymanski et al. 2008). An enhanced understanding of these processes would, however, open the path to improve physically based modelling approaches of actual and future water fluxes (Rothfuss & Javaux 2017). Furthermore, it could help to develop management and conservation strategies to sustain water resources as well as augment eco- and agricultural

system resilience (Penna et al. 2018).

In this study, a laboratory tested membrane based *in situ* sampling method was combined with plant transpiration measurements in a field experiment. We measured the temporal dynamics of the isotopic signature of soil pore water vapour and transpiration of two grassland species under intense dry-wet cycling. For this purpose, we artificially created water limited conditions and applied two heavy rain pulses, each followed by a period of drought. The two pulses differed in their isotopic compositions. One pulse being strongly depleted in both isotopologues and one pulse being heavily deuterated relative to natural abundances. Hence, we were creating a strong contrast between the two water pulses and the pre-existing water in the soil to obtain more unequivocal results (Bachmann et al. 2015, Rothfuss & Javaux 2017). The central objective of this study was to test the applicability of the *in situ* method developed by Rothfuss et al. (2013) under field conditions. We further seek to compare between the new *in situ* and state of the art destructive soil and plant water sampling approaches. The different advantages and limitations of the two methods are discussed in detail in order to enhance future consideration about methodologic approaches to address ecohydrological questions. Finally, we consider the impact of results from the two methods in a Bayesian Isotope Mixing Model (BIMM) (Parnell et al. 2010) on the interpretation of RWU dynamics. This study highlights the necessity to enhance our understanding of the relevance of processes on temporal scales and calls for wider application of coupled soil and transpiration measurements at high temporal resolution.

2 Material and Methods

In the following, Oxygen and Hydrogen isotopic composition is reffered to as ratios between the heavy and light isotopic fraction, relative to the Vienna Standard Mean Ocean Water (Gonfiantini 1978):

$$\delta = (\frac{R_{sample} - R_{V-SMOV}}{R_{V-SMOV}}) * 1000 \quad (2.1)$$

Delta notation of H and O is expressed in (‰).

2.1 Experiment

2.1.1 Principles of gas-permeable tubing and experimental setup

In situ sampling of soil water isotopic signatures was carried out using microporous polypropylene tubing (AccurelPP V8/dHF, Membrana GmbH, Germany; 0.155 cm wall thickness, 0.55 cm i.d., 0.86 cm o.d.) with gas-permeable but hydrophobic properties Rothfuss et al. (2013). The material had originally been developed for microfiltration purposes but has found application in soil atmospheric sampling of CO_2, N_2O and CH_4 (Gut et al. 1998, Flechard et al. 2007, Parent et al. 2013).

The theoretical assumptions of the sampling system are described in detail in Rothfuss et al. (2013) and Volkmann & Weiler (2014). The method can be applied under the assumption of water vapour in soil air-filled pore space to be in isotopic equilibrium with soil water in water filled pore space. The gradient of saturation vapour pressure between interior tube and exterior air-filled porespace drives equilibration of water vapour concentration within a certain time, depending on the strength of the gradient, temperature and the diffusion coefficient of the porous membrane material. In theory, the polypropylene tube is a big soil pore that can be filled with gas but not with water. This technique assumes water vapour to reflect isotopic fractionisation at thermodynamic equilibrium with liquid water. Isotopic signature of the pore water can be calculated back based on temperature measurements with the equation of Majoube (1971). A critical point is the transport of the air volume that is in isotopic equilibrium with the soil air through the tubing system towards the measurement device. It is obtained by applying a flow of dry air on one open end of the tube system that must be lower than atmospheric pressure to prevent disturbance of soil air at sampling location. At the same time, the dry air flow must be higher than the requirements of CRDS analyser, in order to avoid any suction of air through (i) the membrane, (ii) the excess tube or (iii) any leakages of the system due to the low pressure created by the CRDS pump. (Rothfuss et al. 2013)

Rothfuss et al. (2013) have tested the polypropylene tubes to measure soil water stable isotopes under varying conditions in several laboratory experiments. They could show that measurements in sand under controlled conditions were stable and comparable over a range of temperatures (8-24°C), volumetric water contents (0.31-0.09 m^3 m^{-3}) time periods of constant sampling (0.5-4h) and flow rates of dry air (25-100 mL min^{-1}). Tubings did not effect fractionisation on neither of the two isotopes. In their experiments, equilibration time after a change in isotopic composition of water vapour was found to be approximately 5 h (Rothfuss et al. 2013).

In our experiment, we adapted the experimental setup from Rothfuss et al. (2015). Figure 1 (a)

shows the complete field setup, including *in situ* plant transpiration measurement (see Section 2.1.6). In total, 8 membrane tubes of a length of 20 cm (54.8 cm^2 outer, 32.0 cm^2 inner surface area, 4.1 cm^3 inner volume) were extended at both extremities with PFA (Perfluoroalkoxy alkanes) and PTFE (Polytetrafluorethylen) tubing systems (1/4" and 1/8"). Each membrane tube was installed in one specific soil depth. Dry synthetic air flow introduced to the tubes' inlet could be distributed via electric valve manifolds (Oxygen Clean Manifold, Clippard Instruments, Ohio, USA) to a desired tube section from which the respective water vapour sample was transported to the analyzer. Air flow was controlled by a Mass Flow Controler (MFC) (model Tylan FC-260 with a read-out box RO-7010) and always kept sufficiently high to guarantee an excess at system exhaust point.

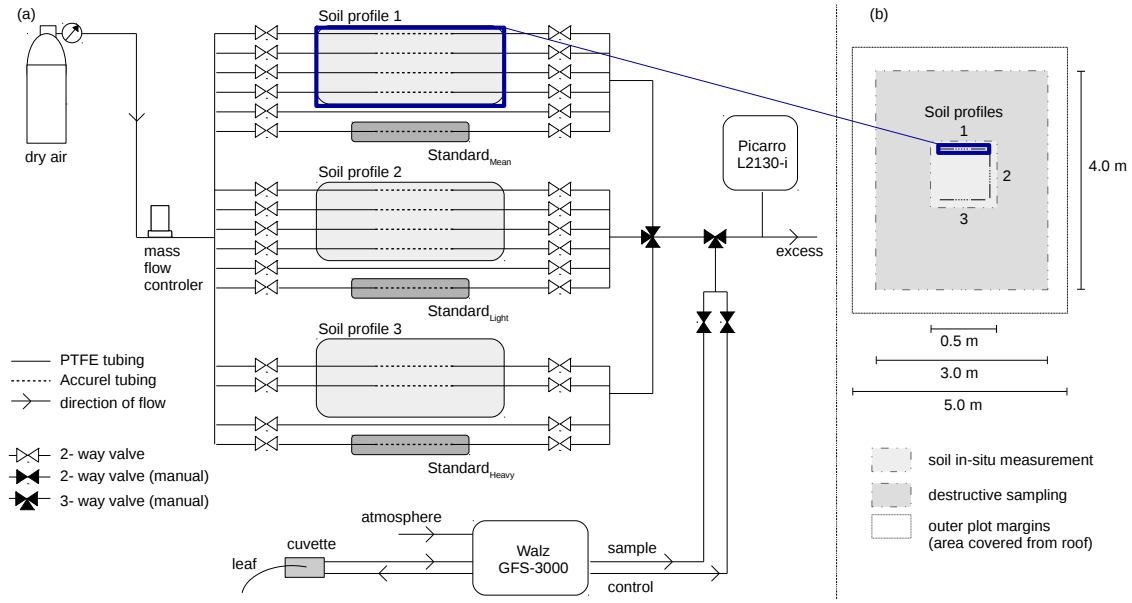

Figure 1: (a) Scheme of the experimental field setup for *in situ* water vapour sampling of soil, ambient air, leaf transpired water and from the three soil water standards (b) Schematic representation of an aerial view of the setup on the experimental field site.

The different tubing compartments were joined with Swagelok (Swagelok Company, Solon, Ohio, USA) or Pargrip (Parker Hannifin Corporation, Richmond, California, USA) connections and the system was tested for air-tightness. Different to Rothfuss et al. (2015), we did not include a dilution line due to the lack of a second MFC.

2.1.2 Preparation of standard vessels for field measurements

Three working standards were used to monitor measurement stability in order to account for instrumental drift due to fluctuating ambient conditions in the field (Volkmann & Weiler 2014, Oerter & Bowen 2017). For this purpose, three vessels were each equipped with one microporous polypropylene tubing with the same dimensions as the tubes that were buried in the soil. Vessels were each filled with 400 ml water of known isotopic composition: distilled tap water ($\delta^{18}O_{VE}$ -9.3 ‰, $\delta^{2}H_{VE}$ -65.3 ‰), one isotopically depleted water ($\delta^{18}O_{L}$ -78.8 ‰, $\delta^{2}H_{L}$ -236.3 ‰) and one deuterated (enriched) water ($\delta^{18}O_{H}$ -9.3 ‰, $\delta^{2}H_{H}$ 865.0 ‰). Isotopic ratios were chosen to cover the isotopical range of the two labeling pulses. All standards were measured against international references and laboratory standards using the vaporizer unit and Picarro autosampler as explained in Section 2.2. Dried sand was added to the vessels until no headspace was left (approximately

1200 ml). Vessel lids were sealed airtight.

All standards were buried in 60 cm depth in the soil at a distance of approximately 4 m from the center of the experimental plot. A temperature sensor was installed between the standard vessels. Insulating material was placed between standard vessel lids and topsoil material to keep changes of temperature of standards as small as possible.

2.1.3 Study site and experimental design

The study was performed at the experimental research site Freiburg Flugplatz in South Western Germany at 238 m a.s.l. (48°01′13"N; 7°49′36"O EPSG 3857). The site represents a temperate, perennial grassland with ruderal vegetation. Mean annual temperature is 11.4°C and mean annual rainfall is 662.1 mm (reference period 1988-2017 *DWD Climate Data Center: Daily climate observations Germany* (2018)). The soil is classified as a skeleton-rich Anthrosol (Kübert, personal communication) on former fluvial deposition and displays pronounced differences between soil horizons. Top layer is brown earth (0-10 cm), followed by a sandy, medium grain gravel layer (10-35 cm) with consolidated clay beneath 40 cm depth. Particle size distribution analysis was conducted for the same location during another experiment (Kühnhammer 2018). Between 0 and 40 cm depth, soil texture consisted of 37.8 % sand, 48,6 % silt and 13.7 % clay. Porosities in the soil ranged between 0.57 [-] in the topsoil and 0.36 [-] in the gravel layer. Dominant species during the time of our experiment were *Agrostis tenius*, *Carex hirta* and *Centaurea jacea*.

In order to test the effect of drought on plant root water uptake, we installed a plot of 4 m x 3 m inner size which could be wrapped up by a transparent rainout shelter in 145 to 210 cm height above the canopy (see Figure 1 (b)). In the center of the plot, 60 x 50 cm earth was excavated. On three sides of the hole, in 2, 5, 20 and 40 cm depth, respectively, the permeable gas sampling tubes were installed . Additionally, soil moisture sensors (10 HS Decagon Devices) and temperature sensors (T108, Campbell Scientific, Logan, UT, USA) were installed in each depth in the wall of the undisturbed soil. Soil excavation material was carefully emplaced trying to imitate original stratifications and eliminate the formation of preferential flow pathways. Sensor data was stored as five-minute averages with a data logger (CR1000, Campbell Scientific, Logan, UT, USA). *In situ* measurement devices were installed on March 26 and natural precipitation was excluded from the plot after June 07. Shelters were set up exclusively before predicted rain events, as well as during the weekend. These shelters included a buffering zone of approximately 100 cm at each side to prevent lateral inflow. Precipitation δ^2H and δ^{18}O values used in this study were part of research on the field site during the previous year (Kübert 2017*b*).

Photosynthetically active radiation (PAR) (S-LIA-M003, Onset, Bourne, MA, USA), air temperature and relative humidity (S-THB-M008, Onset, Bourne, MA, USA) were measured in a distance of 10 m from the experimental site in 1 m height above ground and logged as a five-minute averages (HOBO H21-002 U30, Onset, Bourne, MA, USA). From temperature and relative humidity we calculated vapour pressure deficit (vpd) using the August-Roche-Magnus formula for saturated vapour pressure (Alduchov & Eskridge 1996).

During installation of the setup, two belowground connections of permeable tubes were damaged (Plot 3 in 2 and 40 cm depth) and therefore excluded from the experiment. The final setup comprised a total of 10 measured depths. Pre-tests in the field started on May 18. Measurements from June 15 onwards were included in the results. Figure 2 (*left*) shows a picture of the center of the experimental plot on July 07, during the measurement campaign. As can be seen, the former

Figure 2: *left*: Picture from an aerial view on the formerly excavated area with the buried *in situ* sampling probes beneath on July 07, during the measuring campaign. The three plastic boxes contain the valve systems and mark the places where the tubings come out of the soil. At the top, the leaf cuvette can be seen. *right*: Close-up picture of a leaf of *Arrhenaterum elatius* in the leaf cuvette during measurement.

excavation was not distinguishable from the surrounding undisturbed soil. Plant biomass did not seem to have developed in a different manner.

The soil moisture sensor data was calibrated against gravimetric soil water potential which was determined via soil bulk density and water mass of destructive sampling throughout the whole measurement period.

2.1.4 Irrigation events

By irrigating the plot with labelled precipitation pulses, we intended to increase the gradient between isotopic signatures of different soil horizons. In this way we aimed to achieve statistically robust distinction between different soil horizons despite any occurring measurement inaccuracies or natural occurence of heterogeneity, in order to improve overall accuracies of source partitioning (Seeger & Weiler 2016).

We irrigated the plot two times. The chosen irrigation amounts correspond to rain events classified as "severe precipitation events" and "storm warning", respectively, according to classification of German Meteorological Service DWD (n.d.). Irrigation was applied via a 3 m tubing that was perforated each centimeter with a 1/16" diameter tube. The first irrigation event took place on June 20 between 22:05 and 23:17 h (CEST) with doubly labelled water. A total amount of 240 l was applied on the plot during four cycles of watering, corresponding to a rainfall intensity of 20 mm h^{-1}*m^2. Second rain pulse with deuterated water was applied on July 2 between 22:06 and 23:33 h (CEST). Similar to the procedure during the first watering we applied 240 l in four cycles of eight minutes each. Additionally, another 120 l were applied in two cycles of two minutes each, and 90 l in two cycles of six minutes simulating a rain event of 35 mm*m^{-2}.

Irrigation was performed at night to minimize evaporative losses during tracer application. Nevertheless, due to high temperature of soil and plants, direct evaporation of water was unavoidable.

2.1.5 Protocol of soil isotopic vapour sampling and measurements *in situ*

Soil vapour in each porous membrane tube was sampled on a daily base between 8:30 in the morning and 19:00 (CEST) in the evening. Measurement accuracies of the CRDS instrument are

better than ± 1 ‰ for δ^2H and ± 0.2 ‰ for δ^{18}O. Each measurement sequence started with a flush of valve boxes and tubes with synthetic dry air via bypass lines, adjusting a flow rate of 300 to 700 ml*min^{-1} to evacuate water vapour or condensated droplets of previous measurements in the system. In wet measurement periods, each depth was flushed for five minutes by applying an dry air stream of 300 ml*min^{-1} and followed by an equilibration time of at least 20 minutes. All sampling tubes were sequentially flushed and sampled maintaining in each profile the following order: 20, 5, 40, 10 cm depth. After each membrane tube measurement, the tube system was flushed for five minutes via bypass lines. Measurement duration per porous tube was between 20 and 30 minutes. During drier times, no flushing via sampling tubes was conducted because levels were observed to be stable in the mornings already. Standard vessels were measured once a day, using STD_L and STD_H as last measurements of the day, in order to prevent carry-over (memory) effects in the CRDS instrument.

2.1.6 Plant transpiration measurements *in situ*

Measurements of isotopic signature of leaf water and transpiration comprised two species. We focused on *Centaurea jacea* and *Arrhenatherum elatius* , representating one herbaceous plant and one sweet grass. Both species are perennial and are amongst the most abundant plant species on the field site.

Gas exchange parameters were measured *in situ* with a portable leaf gas exchange system (GFS-3000, Heinz Walz, Effeltrich, Germany) (see Figure 2 *right*). Environmental variables, namely temperature, relative humidity and CO_2 concentration in the leaf cuvette, were set to follow ambient conditions. We used a buffer container to prevent short term effects of plant and human respiration in the CO_2 concentration. Leafs were enclosed in the mornings, and gas exchange parameters were measured during the whole day and stored every 60 seconds. Isotopic signatures of transpiration water and atmosphere were measured several times during the day *in situ* via coupling the GFS with the CRDS instrument. Measurement times during the day were varying due to parallel measurement of soil isotopic composition.

Isotopic signature of transpiration water δ_E in ‰ was calculated via mass balance

$$\begin{aligned} \delta_E &= \frac{u_{out}w_{out}\delta_{out} - u_{in}w_{in}\delta_{in}}{u_{out}w_{out} - u_{in}w_{in}} \\ &= \frac{w_{out}\delta_{out} - w_{in}\delta_{in}}{w_{out} - w_{in}} - \frac{w_{in\,out}(\delta_{out} - \delta_{in})}{w_{out} - w_{in}} \end{aligned} \tag{2.2}$$

with u as flow rate in mol$_{air}$*s^{-1}, w being the mole fraction in mol$_{H_2O}$*mol$_{air}^{-1}$ and δ being the isotope ratio of air with textsubscript denoting incoming and outflowing airstream.

We did not consider the gas exchange parameters and flux rates measured by with the GFS, since it would have exceeded the framework of this master's thesis.

2.1.7 Destructive sampling of soil and leafs for analysis of stable isotopes

Bulk leaf and soil destructive samples were taken on 13 days over the whole period of the experiment. For each species and each depth, three replicates per day were sampled. All samples were taken within distances of maximum 1.80 m from edges of the *in situ* setup (see Figure 1 (b)). At the end of the experiment, soil cores were taken from the space between the *in situ* sampling

tubes to test for an effect of the installation procedure on the soil isotopic composition of the soil water due to changes in soil stratification. Soil cores were taken with a Pürckhauer soil corer (core diameter 20 mm) and stratified into portions of 0-3 cm, 3-8 cm, 12-16 cm, 18-23 cm, 28-33 cm and 38-43 cm depth. During dry periods, sampling was critical due to big losses of sample material caused by the fragility of the soil. Leaf samples of *Centaurea jacea* were sampled from three different plant individuals. Midrips were cut out, and only veins and lamina were used as sample material. *Arrhenaterum elatius* samples comprised several leaves to guarantee the availability of enough liquid for analysis. Leaf samples were always taken between 14:30 and 15:00 h. Soil samples were taken afterwards, usually within a timeframe of two hours. Immediately after sampling, samples were inserted into a gas-tight 10-ml septum-capped glass vials, kept in a cool box during transportation and stored at 4°C until further analysis.

2.1.8 Cryogenic vacuum extraction and measurement of liquid water

The cryogenic vacuum extraction system comprised four separate extraction units, each with five extractioncollection lines. Each unit had a separate independent valve, and system pressure could be tested individually easing the detection of leakages. Before the extraction procedure, air was evacuated from pipe system by applying a negative pressure of 1 to 10^{-1} mbar with a vacuum pump (XDS10, Edwards, Burgess Hill, UK). Afterwards, sample vessels were heated up to 95°C and evolving water vapour was caught in glass tubes plunged in liquid N_2 cold trap for 90 minutes. Samples were defrosted at room temperature under sealed conditions until water could be pipetted into 1.5 ml thread vials (ND9, LLG, Meckenheim, DE) with closed lids. Water samples were stored at 4°C until analysis in the CRDS. Water recovery rates were determined via pre- and post-ovendried (120°C for 48 h) soil sample weights.

Analysis was conducted with a PICARRO vaporization module V1102-i coupled to a robotic A0325 autosampler and then measured with the same CRDS device which was used in the field.

2.2 Data processing and calibration

2.2.1 Time series signal processing

An automated processing system was implemented in R (R Core Team 2017) to identify stable measurement plateaus based on the valve control unit log file and field notes. Inspecting the time series of CRDS measurement (see Figure 4) individual sample sequences can be easily identified by visual inspection. In the measurement of different soil depths, water vapour concentrations and water isotopic signatures showed the characteristic behaviour of asymptotic convergence towards a stable level. As Volkmann & Weiler (2014) analyzed in their experiment, this behaviour can "be primarily attributed to advective–diffusive reactive transport through the soil pore space and the various segments of the probing system as well as storage effects such as cavity reservoir gas exchange.". The first two and the last minute of each individual measurement were discarded to account for transport time of sample and storage effects in the tubes. Using data of soil temperature from sensors in the respective depth, the equation for free water liquid–vapour equilibrium fractionation established by Majoube (1971) was applied. Then, rolling averages of coefficient of variation (CV) over three minutes were calculated and the time of most stable measurement was chosen based on equation 2.3.

$$CV^{x}_{weighted\ min} = min(1\ CV^{x}_{\delta^{18}O}\ +\ 0.5\ CV^{x}_{\delta^{2}H}\ 0.5\ CV^{x}_{H_2O}) \tag{2.3}$$

Standard deviations of identified plateaus greater 0.3 ‰ or 1 ‰ for δ^{18}O and δ^{2}H, respectively, were flagged. The influence of water vapour mixing ratios on isotopic composition was corrected via measurement of standard vessels, as recommended by Schmidt et al. (2010) (see Figure A.3 in the Appendix).

Standardization of field measured values was conduced by calculating linear regressions between isotopic composition $\mathrm{STD_{required}} \sim \mathrm{STD_{actual}}$. On June 21., July 07. and July 07. measured standards were excluded from data calibration due to fluctuations during the measurement. Standardization was conduced instead by interpolating linearly between correction coefficients of the previous and the following day, respectively.

2.2.2 Measurement protocol and calibration of measurements with vaporization module

Measured values of extracted liquid water were corrected via measurement of three in-house reference water standards ($\mathrm{STD_H}$, $\mathrm{STD_M}$, $\mathrm{STD_L}$) that were calibrated against primary international reference materials (VSMOW2, GISP, and SLAP2) (IAEA, Vienna). Nine standard samples (three replicates per standard) were measured at the beginning of each autosampler measurement series, usually comprising 40 samples. Additionally, one replicate of medium range standard was measured after ten samples to account for any changes in the measurement conditions, e.g. room temperature, during the cycle.

For data calibration, we did not use the provided standard software ChemCorrect$^{\mathrm{TM}}$ from PICARRO. Instead, we implemented calibration procedure similar to the approach from Van Geldern & Barth (2012) since we expected problems due to memory effects in case of high absolute differences of delta values ($\Delta\delta$) (Van Geldern & Barth 2012, Penna et al. 2012). Memory coefficients were calculated with equation 2.4.

$$m^{n}_{i} = \frac{\delta^{(n-1)}_{t} - \delta^{n}_{i}}{\delta^{(n-1)}_{t} - \delta^{n}_{t}} \tag{2.4}$$

Coefficients were calculated as differences between $\mathrm{STD_L}$ and $\mathrm{STD_M}$ for 18 injections.

Memory correction was only applied to samples that had experienced the second labeling pulse (strong deuteration) since we did not observe amelioration of values in ambient range, when $\Delta\ \delta$ were low. Highest $\Delta\delta$ during the measurement were 46.1 ‰ for δ^{18}O, and 402.1 ‰ for δ^{2}H respectively.

Memory coefficients were changing over time, varying from 0.90 to 0.98 for injection number 6, meaning that the analysed isotopic value represented 90 and 98 % of the true sample value (Van Geldern & Barth 2012). Measured values of laboratory standards at the beginning of each tray were corrected via simple linear dependencies of *measured* $\sim$ *nominal*. All linear regression models showed to be strongly correlated ($R^2 > 0.99$) and highly significant ($p < 0.001$). The resulting linear functions were applied to correct all measured values of samples within the specific measurement cycle. Linear relationship of changes in measurement of $\mathrm{STD_{M\ measured}}$ relative to $\mathrm{STD_{M\ nominal}}$ over each measurement series was calculated as linear relation from time difference.

Time dependant correction factors for each sample were calculated accordingly and the offset was cleared from the prior calibrated value.

Mean long term analytical precision, calculated as mean difference between $STD_{M\ target}$-$STD_{M\ measured}$ of raw values and after correction procedure are presented in table 1. For a graphic representation see Figure A.4 in the Appendix.

Table 1: Mean and sd of CRDS measurement precision of liquid sample measurement raw and after correction procedure.

	$\delta^{18}O$		$\delta^{2}H$	
	mean	sd	mean	sd
raw	0.50	1.21	-0.93	3.4
corrected	0.13	0.19	1.09	1.8

2.3 Data analyses

All data analyses were carried out using the programming and statistical language R version 3.4.4 (2018-03-15) (R Core Team 2017).

2.3.1 Statistical analyses and evaluation

Dual-isotope grafical representation was used to compare between processed *in situ* and destructive laboratory-based isotope measurements. Linear regression analysis was employed to evaluate temporal trends and effects of evaporation on soil, plant and atmosphere water pools over the course of the experiment.

A target standard deviation for acceptable performance was set to ± 0.2 ‰ for $\delta^{18}O$ and ± 2 ‰ for $\delta^{2}H$ for *in situ* and laboratory standard measurements (Orlowski et al. 2016, 2018). Propagation of errors associated with the extraction method, or variables such as soil weighting, temperature measuring precision were not taken into account due to the overall high workload within the framework of the present thesis. Results of transpiration measurements are reported as replicate mean with associated standard deviations.

In order to test whether isotopic compositions of soil horizons obtained by the different methods were drawn from the same distributions, the non-parametric Mann-WhitneyWilcox test for statistical significance at a 95% confidence interval ($p \leq 0.05$) was conducted. Similar to the procedure described by Millar et al. (2018), Dunn's test was performed to examine, whether soil horizons during the different phases of the experiment were statistically differentiable. As false discovery rate control, the Benjamini-Hochberg method with p-value adjustments was used. Tests were performed for both water isotopologues separately.

2.3.2 Transpiration water

The isotopic signatures measured *in situ* by the gas exchange system coupled to the CRDS are reflecting transpiration water, whereas data from extraction analysis is representing bulk leaf water isotopic composition. Sampling of lignified plant parts of herbaceous vegetation in order to measure directly source water values was not possible due to insufficient availability of herbaceous plant material on the experimental site, as well as the usage of a highly destructive sampling

procedure. Therefore, in order to enable comparability between the two methods, isotopic signature of transpired water based on results from destructive method had to be modeled. We used the fractionation model of evaporation developed by Craig & Gordon (1965) (equation 2.5). The model can be used under the assumption that transpiration has achieved isotopic steady state. In this case, isotopic composition of transpired water equals the value of source water (Ehleringer & Dawson 1992).

$$R_E = \frac{1}{\alpha_k \alpha^+ (1-h)} (R_e - \alpha^+ h R_a) \tag{2.5}$$

R_E being isotope ratio of transpiration water, R_e and R_a are ratios of bulk leaf water and the atmospheric water vapour. Isotopic ratios can be converted to delta notation by $\delta = \mathrm{R} - 1 * 1000$. Variable α_k is the temperature sensitive equilibrium fractionation factor which was calculated via atmospheric air temperature with the equation of Majoube (1971). The kinetic fractionation factor α^+ reflects the impact of surface boundary conditions (Merlivat 1978) and h denotes relative humidity corrected for air temperature.

2.3.3 Estimation of root water uptake depth

Plant water uptake occurs not linearly, as uptake of water in one specific soil depth, but has to be understood as the integral signal of all depths within the soil where roots are active. Hence, multi-source mixing approaches are conceptually better suitable than linear interpolation methods (Parnell et al. 2010, Prechsl et al. 2015, Sprenger et al. 2016). Based on multi- source mixing approach, several models exist. Here, we are making use of SIAR (Stable Isotope Analysis in R), developed by Parnell et al. (2010), since it (i) enables inclusion of variability of the input parameters due to Bayesian approach, (ii) enables the work with underdetermined systems (iii) quantifies the likelihood of sources (iv) is easy applicable for R-users (Parnell et al. 2010, Phillips & Gregg 2003, Evaristo et al. 2017, Parnell & Jackson 2013). SIAR allows incorporation of (external) prior-distributions which account for e.g. system variability or measurement uncertainty. Default distribution is Dirichlet distribution, a generalisation of the Beta-distribution. The source associated variablity and uncertainty are assumed to be normally distributed but they are designed to be vague to keep a high influence of data on the results (Parnell et al. 2010, Evaristo et al. 2017). In an iterative procedure, a Markov chain Monte Carlo fitting algorithm approaches the observed end-member values. Model output are posterior distributions with estimated parameter values of contributions of each source.

For our project, we used four input combinations. Input sources were *in situ* and *ex situ* measured mean daily isotopic compositions of soil water (two combinations, each with four possible sources). Input end-members were *in situ* and *ex situ* results of mean daily isotopic composition of plant transpiration for *C. jacea* and *A. elatius*, respectively. To foster model performance, data for both water isotopes were used.

The model parameters were set as follows: iterations = 200 000, burning = 50 000, thinning = 15, trophic enrichment factor = 0. For better interpretation, we aggregated simulated posterior distributions (probability density functions) in blocks of 1 % source contribution fractions and calculated a most frequent value (mfv). Since the model is constrained to the sum of all fractions being 1 (100%), the combination of values closest to their mfv was drawn from the four posterior distributions.

3 Results

3.1 *In situ* ambient conditions and measurement of soilwater $\delta^{18}O$ and $\delta^{2}H$

3.1.1 Evolution of soil water content, temperature and relative humidity

An overview over climate parameters relevant within the time of our experiment is given in Figure 3. We observed only four minor precipitation events during the time of drying of the soil, the heaviest of which was 9 mm and occurred on July 05. Water vapour pressure deficit (VPD) showed clear diurnal pattern, following air temperature (not shown) and ranging from values around 0 kPa at night, and 6.1 kPa during middays.

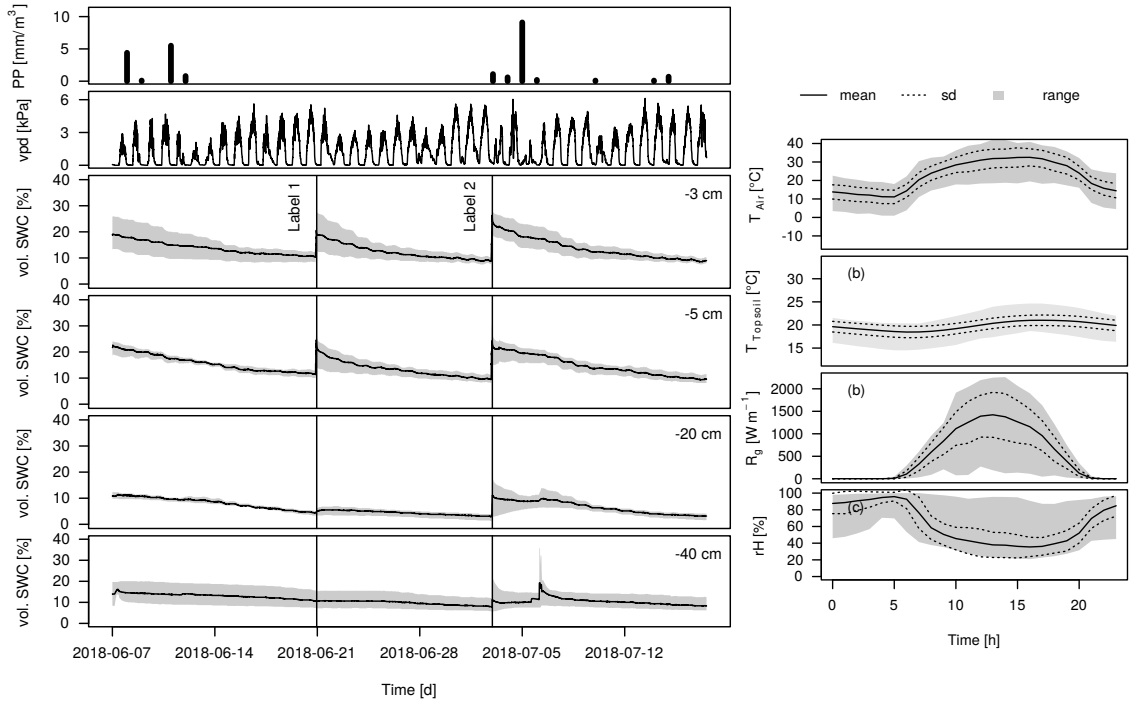

Figure 3: *left*: Evolution of precipitation, vpd and soil water contents within the different depths during the course of the experiment. *right*: Daily cycles of air and topsoil temperature, global radiation and rH during the measurement campaign (18.06.-17.07.).

The effect of the shelters is clearly visible in calibrated volumetric soil moisture (θ_v). Moisture declines during the drying period in all depths and increases after the application of each labelling pulse. Slopes are steepest in the two upper soil horizons, whereas lower horizons show less reaction on labelling input and overall more stable θ_v. Higher variety of θ_v between replicates was measured in the topmost soil layer as well as in -40 cm depth and after each applied precipitation event. After the above mentioned rainfall event on July 05, a short peak is observable in the two deeper soil horizons. The highest θ_v median was measured in -5 cm and the lowest SWC is observed in -20 cm depth. Except for the peak value in -40 cm, highest differences of soil moisture during the measurement period were observed at -3 cm, with values ranging from 36 % in 7 %.

The prevailing development of air temperature during the day was characterized by a strong increase from 11.1°C at 5 am in the morning, reaching a stable maximum at midday of around 31.2°C, before declining slowly towards the evening again. Topsoil temperature followed the same

pattern although amplitude was less pronounced and approximately 2 h delayed from the air temperature, reaching the mean temperature maximum of 22.0°C around 6 pm.

Evolution of subsoil temperatures is displayed in Figure A.1 in the Appendix. Daily temperature amplitudes were strongest in topsoil and decreased with increasing depth. Spatial variability between the three measurement probes was found to amount ± 1.3°C in 3 cm depth and only ± 0.25°C in 40 cm depth

Global radiation was highest at 1 pm reaching mean intensities of 1422.4 W*m^{-1}. Relative humidity was inversely related to temperature, reaching its mean daily minimum of 35.5 % around 4 pm whereas maximum values of 94.7 % could be observed around 5 am in the morning. Daily ranges differed strongly also during midday, reaching up to 95.0 % after rain events whereas before the second labeling pulse, rH amounted only 20.8 %.

3.1.2 Example of a measurement sequence

Figure 4 shows the measuring sequence of DoE 27, giving an example of the daily measurement routine. With the opening of a valve, signals of all parameters (wvmr, $\delta^{18}O$, $\delta^{2}H$) were following a similar pattern of sharp transition, followed by a convergence towards a stable value. The $\delta^{18}O$ signal needed a longer equilibration time until the plateau was reached. The time required to reach stable values depended on several factors, such as magnitude of difference between isotopic signatures of two subsequent measurements, temperature difference between soil and atmosphere, sampling depth. Plateaus were more stable in dry periods, but after application of rain pulses, however, values were more afflicted with uncertainty due to signal variation. Measurements that remained unstable were excluded from the results because of possible condensation effects.

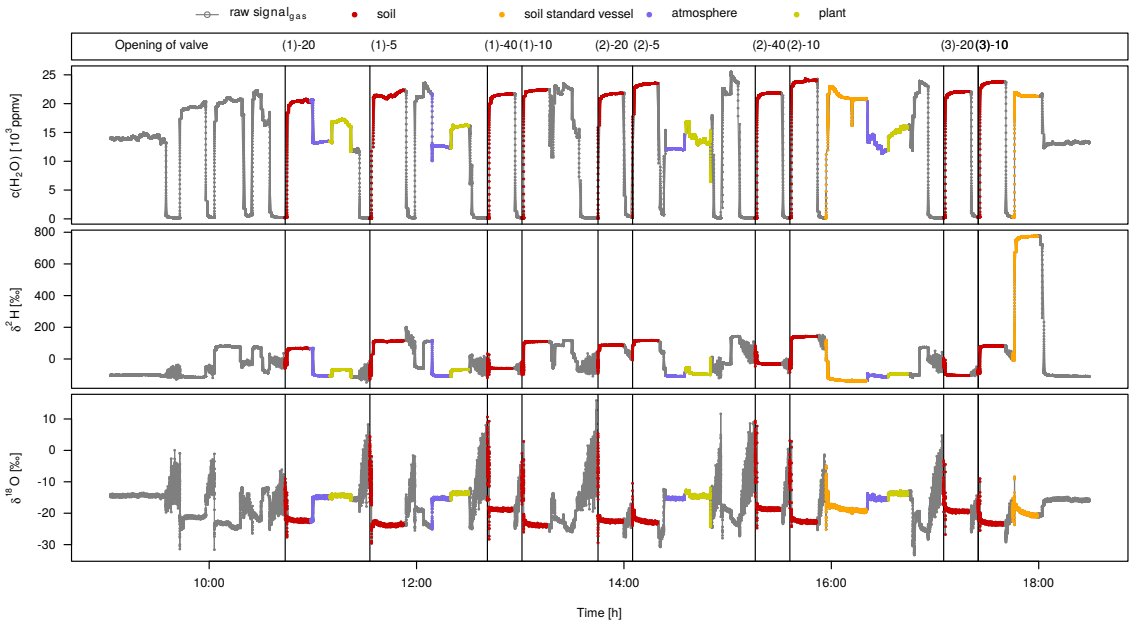

Figure 4: Examplary time series of a daily measurement sequence on DoE 27, illustrating the acquisition of soil pore and transpiration water vapour values of (a) water vapour concentration, (b) $\delta^{2}H$ and (c) $\delta^{18}O$ using the *in situ* sampling technique. Grey sections were not used for further analyzation whereas colored sections represent individual sampling phases of different soil depths, soil standard vessels, atmosphere and leaf transpiration. Vertical lines are indicating the opening of magnetic valves before a valid measurement at a specific soil depth.

Dry air flushing of tubes can be easily identified as measurements with water vapour mixing ratios below 1000 ppmv. From the different sampled water compartments, the water vapour

mixing ratios of atmospheric samples was lowest with mean values of 16000 ppmv, ranging from 12000 to 24000 ppmv. Soil and standard water vapour mixing ratios ranged between 17000 and 25000 ppmv and showed to be very stable during measurement. Transpiration vwmr showed to be most unstable, varying from 12000 to 30000 ppmv.

An overview over deviation of reference measurements of standards is given in Figure A.2 (Appendix). No apparent drift in standard isotopic composition was observed. Linear relationship between measurement water vapour mixing ratio and standard δ^2H measurement precision was weak ($R^2 = 0.31$) but significant ($p<0.01$) and was corrected accordingly for all soil measurements (see Figure A.3 in the Appendix).

3.1.3 Temporal evolution of δ^{18}O and δ^2H in soil profiles

Depth profiles of pore water isotopic composition measurements obtained from *in situ* measurements are presented in Figure 5 separately for all three replicates. Results are physically plausible and we observed good conformity between the three replicates. Analytical precision determined as mean variability (cv) within each measurement in the field was 0.8 % for δ^{18}O and 0.07 % for δ^2H. Mean CRDS accuracy based on medium standard measurements amounted to 0.29 ‰ deviation from target value of δ^{18}O and 5.3 ‰ in δ^2H (see Figure A.2 in the Appendix). This expresses the average correction applied on values from soil measurements.

At Pre-conditions (DoE 1-5), $\delta_{S\,liq}$ showed typical exponential shape with strongest enrichment of both isotopologues in 3 cm depth and gradual depletion in deeper horizons. Measurement sd is somewhat too high in this horizon to distinguish between temporal dynamics. Only in 20 cm depth, daily results can be separated unequivocally from another. The first pulse of labelled water led to decrease mean signatures of both isotopologues in the topsoil within 12 h by nearly an order of magnitude from -6.4 to -43.3 ‰ (δ^{18}O) and -40.4 to -145.1 ‰ (δ^2H) between DoE 5 and DoE 6.

In 20 cm depth, the signature was still affected but composition in 40 cm depth was changing only in small orders of magnitude. Profile 3 supports the observations from the other replicates at 5 cm but differs consistently in the results obtained at 20 cm depth. During the course of the experiment, the effect of topsoil evaporation was observable as an enrichment of both $\delta_{S\,liq}$ relative to the previous day. In profile 1, -3 and -5 cm were affected in a similar magnitude by the effect, whereas in profile 2, enrichment in -3 cm increased relative to -5 cm depth from DoE 8 onwards. Another distinct temporal pattern is observable at -20 cm, where in contrast to the other profiles, isotopic composition seems to decrease in profile 2 between DoE 12-14. All observations during the first labelling phase are notable in both $\delta_{S\,liq}$.

The second labelling event increased δ^2H concentration (on average from -97.1 ‰ to 271.5 ‰) while δ^{18}O was shifted back towards values in the range of natural abundances (from -25.5 ‰ to -13.7). Different from the first applied rain event, $\delta_{S\,liq}$ 40 cm depth drifted out of natural abundance range. Again, isotopic composition in -3 cm depth was found to shift faster towards pre-event values in profile 2, whereas in profile 1, isotopic composition of both topsoil layers underwent more steady depletion. At the end of the experiment, δ^{18}O values over the whole profile differed only by 4 ‰ between top- and subsoil. Mean δ^2H within the profile remained augmented relativ to natural abundances, with 158.1 ‰.

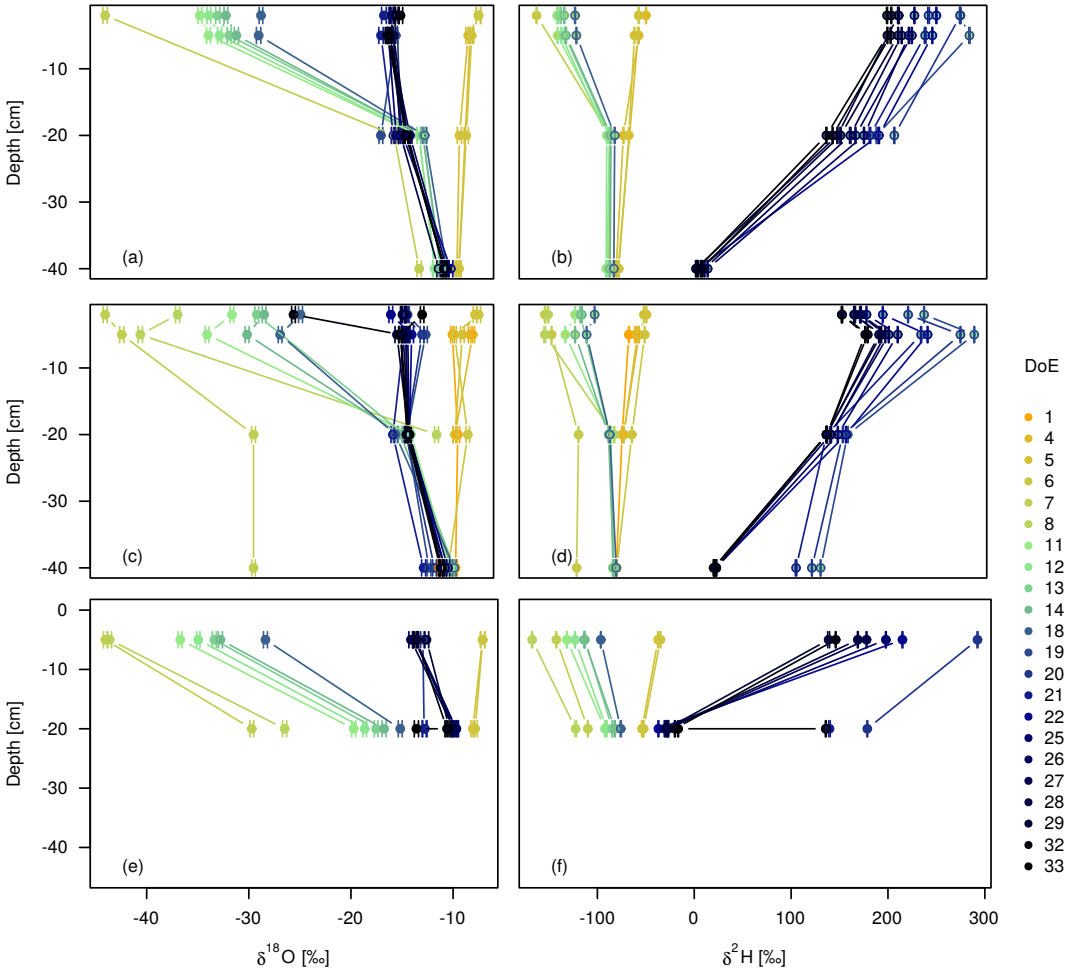

Figure 5: Development of soil isotopic composition in soil profile 1 (a,b), profile 2 (c,d) and profile 3 (e,f) over the course of the experiment. The colours are representing evolution of soil isotopic composition. Application of labelled water was performed during the nights of DoE 6 and 19. Left panels (a,c,e) display dynamics of $\delta^{18}O$, right panels (b,d,f) display $\delta^{2}H$ of water within the different depths of the soil profiles. Errorbars show stability of the individual measurements averaged over the period considered as most stable conditions.

3.1.4 $\delta^{2}H$ and $\delta^{18}O$ relationships in soil water and atmosphere water vapor

Each plot in Figure 6 represents data of one labelling event. Water isotopic relationships of pre-event conditions, atmospheric water vapour and precipitation water of previous year are shown in both panels. The global meteoric water line (GMWL i.e. slope = 8) is also represented as a reference. The local meteoric water line (LMWL) has an intercept of 8.6 with a linear regression slope (LRS) of 7.8. Linear regression through data points of atmospheric water vapour signatures was significant with $p < 0.01$ but R^2 amounted to 0.64 only. Values were enriched relative to liquid precipitation isotopic composition and had a lower regression slope of 7.0 at overall higher scatter.

At natural conditions, soil water isotopic composition had undergone a stronger enrichment in ^{18}O than ^{2}H relative to local precipitation, resulting in a LRS of 6.4 ($R^2 = 0.6$, $p < 0.01$). After application of the first dual-isotopic labelled rain pulse, LRS of the overall profile was 2.5 (DoE 7, $R^2 = 0.99$, $p < 0.01$) and decreased to 2.2 on DoE 18 ($R^2 = 0.98$, $p < 0.01$) before application of the second rain pulse during the night. On DoE 19, 12 h after the irrigation with deuterated water, linear relationship between both stable water isotopes in the soil profile was not significant (DoE 19, SLR = -5.0, $R^2 = 0.01$, $p > 0.5$). Only by the end of the second labelled pulse, correlation was significant again and LRS was -37.5 (DoE 33, R^2 0.69, $p < 0.05$).

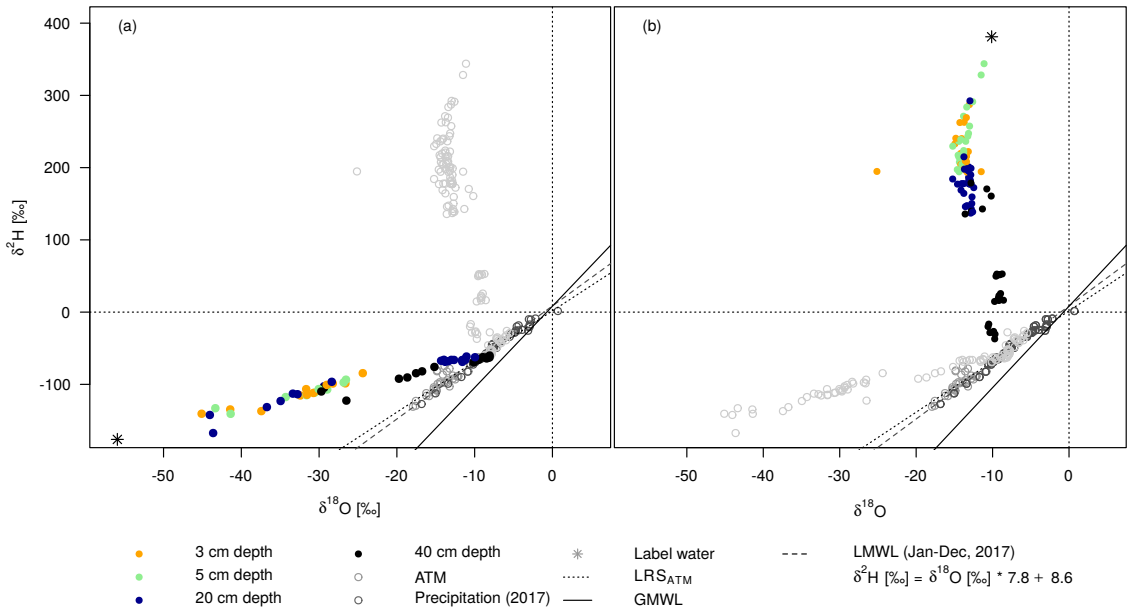

Figure 6: $\delta^{18}O$ and $\delta^{2}H$ from *in situ* measurement in dual isotope space. Couloured points in panel (a) display measurements of all depths of the three replicates after first labelled irrigation pulse. The same is shown in panel (b) after the second labelling pulse. Isotopic signatures of natural precipitation (2017), measurements of atmospheric water vapour isotopic composition and values from soil water at pre-conditions are also displayed in darkgrey. Lines are marking GMWL, LMWL and linear regression from atmospheric vapour isotopic values.

3.2 Comparison of *in situ* and extraction method

3.2.1 Soil water measurements

In Figure 7 soil water $\delta^{18}O$ and $\delta^{2}H$ from *in situ* measurements and vacuum extraction analysis are plotted in dual isotope space. For better comparison, $\delta_{PP\ 2017}$ and $\delta_{ATM\ liq}$ are also displayed. The least squares regression through *in situ* soil water vapour specimen shows a LRS of 8.2 ($R^2 = 0.60, p < 0.001$), which is very similar to LMWL (LRS = 8.56). All measured values lie within the ranges of precipitation isotopic signature of the previous year and the $\delta_{ATM\ liq}$ measurements during the experiment. In contrast, least square regression through vacuum extracted soil samples shows a slope of only 5.6 ($R^2 = 0.88, p < 0.001$) and there is a clear offset between the results of the two methods.

The difference between the means of the methods amounts to 13 ‰ for $\delta^{2}H$ and to 0.9 ‰ for $\delta^{18}O$.

Considering only soil water values in 20 and 40 cm depth, the LRS of both methods are very similar with 6.34 (*in situ*) and 6.44 (CVE) ($R^2 = 0.65$ resp. 0.85, both $p < 0.001$). The offset is approximately 13.5 ‰ in $\delta^{2}H$.

The dual-isotope plots of Figure 8 display all *in situ* and destructively obtained samples after irrigation events separately based on the soil depth that they originate from. Again, GMWL and LMWL and $\delta_{PP\ 2017}$ are shown as reference. Topsoil *in situ* measured isotopic signatures show the highest enrichment and clusters of varying relationship between the heavy isotopes during the two labelling periods are visually distinguishable. The isotopic composition of labelled $\delta_{S\,liq}$ in dual isotope space shows as nearly linear patterns between labelling the pulse and isotopic signatures at natural abundances. Regarding similarities between isotopic compositions of irrigation water and measured samples, the greatest correlation is found at 5 cm depth for the in situ method

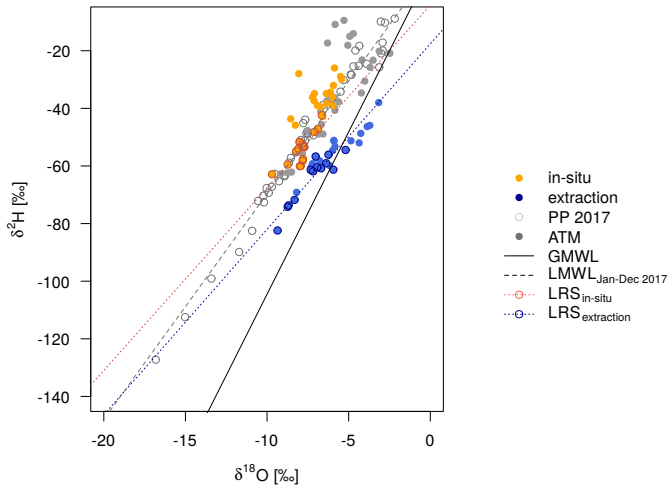

Figure 7: Comparison of soil water $\delta^{18}O$ and $\delta^{2}H$ analysis from *in situ* sampling and cryogenic vacuum extraction at pre-event conditions from all horizons in dual isotope space. Precipitation and measurements of atmospheric water vapour isotopic composition are also displayed. Lines are marking GMWL, LMWL and linear regression between $\delta^{18}O$ and $\delta^{2}H$ from both methods at -20 and -40 cm depth.

whereas the extraction method showed slightly better correlation at 3 cm depth. Values obtained by vacuum extraction analysis in the upper centimeters are consistently lower than the *in situ* measured values and are more scattered after the second irrigation.

Analyses with the Wilcoxon signed rank test showed differences between the methods to be statistically significant at pre-event conditions with $p < 0.05$. Statistically significant differences between the methods, differenciated by soil depths, were found after the first irrigation event only for $\delta^{18}O$ in 40 cm depth. After the second labelling pulse, statistically significant differences were observed between $\delta^{18}O$ values of CVE and *in situ* probes in 3 cm depth and between $\delta^{2}H$ values in all depths.

During all periods, *in situ* measured $\delta^{2}H$ of the two upper (-3, -5 cm) and the two lower soil layers (-20, -40 cm) showed to be significantly different, according to Dunn's test. $\delta^{18}O$ values however, were at pre-event conditions only statistically different between -3 and the lower layers. In contrast, after the first and the second labelling event, only differences between -3 and -5 cm were still not significant. Group differences of CVE results are similar for preconditions, (-3 cm $\neq$ -20 and -40 cm). But Dunn's test results evaluate the labelling to not have contributed to statistically robust differences between the layers for the CVE results.

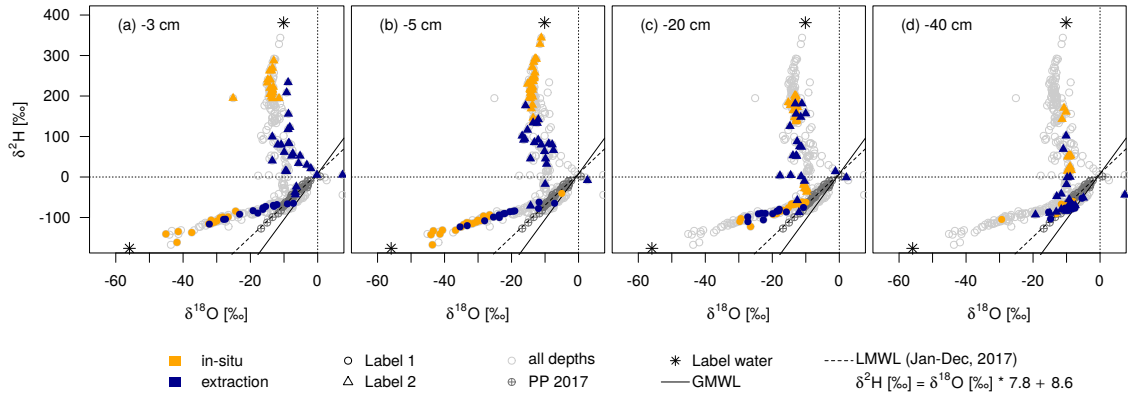

Figure 8: $\delta^{18}O$ and $\delta^{2}H$ of *in situ* and destructive sampling in dual-isotope space. The panels a,b,c and d are displaying observations in -3,-5,-20 and -40 cm depth, respectively.

A graphical presentation of depth distribution of soil isotopic composition from CVE samples taken within the former excavated material compared to samples drawn on the same date from the undisturbed surrounding soil is given in Figure A.5 in the Appendices. $\delta^{18}O$ measurements showed to have an offset of 10 ‰ at upper soil layers. Since the last *in situ* measurements were available only from two days before soil cores for comparison were taken, only samples from deeper soil layers are assumed to be representative for the comparison, because they are assumed to be less influenced by evaporation. At -40 cm, differences between the methods as well as the different sampling points amount to only 1 ‰ and are therefore negligibly small. Our results for $\delta^{2}H$ support the above described findings. $\delta^{2}H$ values in subsoil from the refilled material lie within the ranges of *in situ* sampling as well as CVE probes from undisturbed soil. Soil layers closer to atmosphere have show higher depletion in $\delta^{2}H$ in the refilled material ranging from 13.4 (-3 cm) to 72 ‰ (-8 cm) depth.

3.2.2 Plant water measurements

Figure 9 displays temporal evolution of transpiration isotopic signal of *Centaurea jacea* and *Arrhenatherum elatius*. Destructively obtained samples from test sampling prior to the experiment were included due to loss of samples from DoE 5 during extraction analyses. Temporal patterns of plant transpiration and response magnitude determined with the two methods are strikingly different. Offset of water isotopologues between the results of the two methods at pre-event conditions amounts 4.6 ‰ for $\delta^{18}O$ and 48.9 ‰ for $\delta^{2}H$. However, both methods find similar transpiration isotope signatures of both species prior to the experiment. During this period, the transpired water of *A. elatius* and *C. jacea* from CVE and *in situ* analysis are differing only by 1 and resp. 1.1 ‰ in $\delta^{18}O$ and by 4.4 and, respectively, 17.2 ‰ in $\delta^{2}H$. Considering measurement precision and model error, significant distinction between the results is not given.

Both species show responses after the applications of the two rain pulses. Changes towards more negative isotope composition are visible in both plants within 15 h after application of the first labelling pulse.

Irrigation with the dual labelled water was followed by increasingly negative responses in $\delta^{18}O$ of the *C. jacea* transpiration vapour isotopic signature that could be observed with both methods. From DoE 11 onwards, the transpiration rose again 6 days after the rain pulse, followed by a decrease observable in all bulk leaf waters of CVE analysis and the modelled transpiration values. All CVE results show a sharp peak in both isotopologues of both plants on DoE 20, followed by an immediate drop towards values in the range of DoE 19 or below and a steady increase of the transpiration isotopic signature until the end of the experiment. GFS coupled *in situ* measurements of $\delta^{18}O$ in *C. jacea* transpiration water also detected most pronounced changes on the days after the application of deuterated water, but controversely to CVE findings, we only observed a steady decrease of $\delta^{2}H$ values in *A. elatius* transpiration water. *In situ* measured *C. jacea* $\delta^{18}O$ transpiration water values were showing similar patterns after the first and the second application of rain pulse.

GFS transpiration measurements are systematically more enriched in both water isotopologues than modelled water vapour from bulk leaf signature. These findings are clearly visible also in the dual isotope space and are particularly pronounced for $\delta^{2}H$ in the period following the second irrigation event (see Figure A.6 in the Appendix).

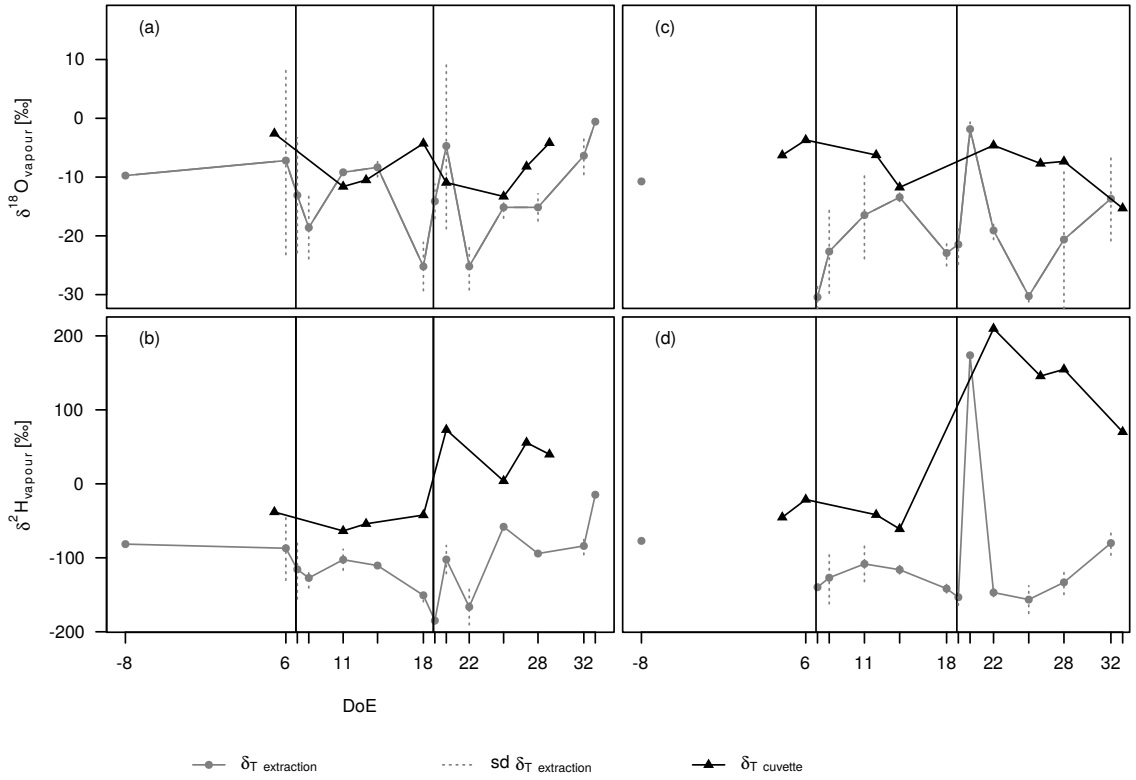

Figure 9: Comparison of transpiration signature for *left* δ^2H and *right* δ^{18}O of *Centaurea jacea* (a,b) and *Arrhenatherum elatius* (c,d). *In situ* measurements are based on isotopic compositions of water vapour from single leaf cuvette measurements. Destructive sampling transpiration signals were modelled from bulk leaf samples and reflect mean isotopic comosition of several leaves per sample and 3 samples per day. The vertical lines are marking dates at which labelled rain pulses were applied.

3.3 Comparison of estimates from multi source mixing models

Results of Bayesian Multisource Mixing Model (BIMM) indicate that, of all combinations the highest probability (mfv) of plant uptake depth occurs at -40 cm with the highest daily fractions of uptake amounting to 91.1 % in *Arrhenaterum elatius* and 70 % in *Centaurea jacea*. Apart from this result, consistency in the resulting probability distributions of rootwater uptake depth between the models is poor.

Results of BIMM with *in situ* measured input distributions are presented in panel (a) and (b) in Figure 10. Five days after the first rain pulse, the fraction of water uptake in the topsoil amounts to 10.6 % and 7.5 % and steadily declines to 5.7 and 6.5 % from *C. jacea* and *A. elatius*, respectively. The decline of water share of topsoil in *C. jacea* goes along with a shift towards 20 cm as water source, the latter is contributing up to 37 % of total uptake. In contrast, *Arrhenaterum elatius* increases its water supply from -40 cm, accounting for 80 % of the total water consumption during this period. After the second labelling pulse, both plants draw water again increasingly from -3 and -5 cm depth. Maximum water uptake from shallow soil then accounts to 28.6 % of water use from *C. jacea* and 27.5 % of *A. elatius* on DoE 25/26, seven days after the event. Contrarily to the uptake dynamics after the first rain event, *A. elatius* also augments uptake from 20 cm depth, while *C. jacea* obtains water from the deepest layer.

BIMM with input data from CVE differs substantially in the estimation of the shares of upper and deeper soil layers (Figure 10 panel (d)). Mfv of *A. elatius* uptake depths of CVE over the course

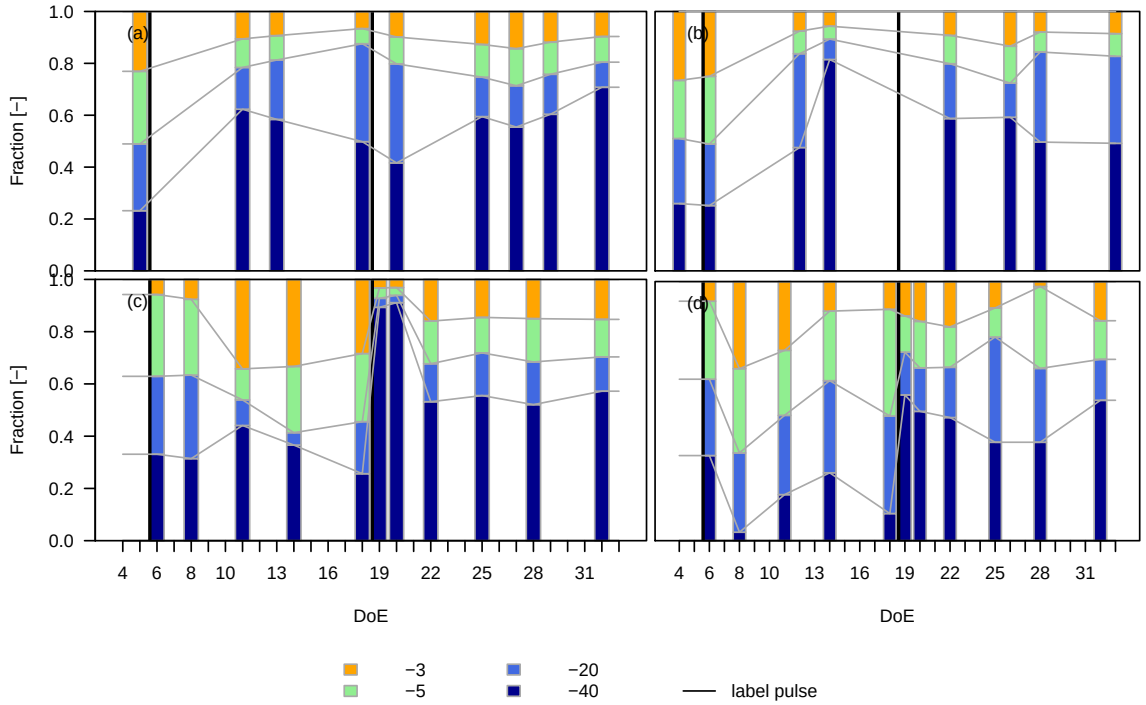

Figure 10: Most frequent value (mfv) of water uptake depth distribution as proportion of the total transpired water from *left: Centaurea jacea* (a,c), and *right: Arrhenateum elatius* (b,d). The upper row shows BIMM results with *in situ* sampling methology, below, values from destructive sampling methology were used as model input.

of the experiment differ from all other input combinations, estimating the proportions of water uptake from upper two horizons to be 35.5 %. Conversely, all other model results resume uptake in the uppermost cm of soil to contribute only 18.9 ± 2 %. The temporal dynamics of uptake by the grasses support the findings of the comparative *in situ* model, proposing an increased uptake from the upper soil depths directly after irrigation and a steady decrease within the following weeks. The maximum response in uptake from 3 cm depth is calculated to occur already after three days, instead of seven. Model estimates of uptake dynamics from *C. jacea* with CVE as input data finds source water fraction from 3 to 5 cm depths to be highest between DoE 10 and 17, with a maximum share of 57 %. Then, on DoE 18 and 19, this share decreases suddenly towards 6 % before rising again three days after the second irrigation towards a stable estimation of 15.1 ± 1.5 % contribution from each of the two shallow horizons.

4 Discussion

4.1 Evaluation of membrane tube sampling technique for soil measurements

4.1.1 General considerations

The aim of this study was to test an existing laboratory setup to monitor soil water isotopic composition under field conditions. Results were further combined with *in situ* measurements of plant transpiration and compared with results from an established destructive sampling method.

Our *in situ* measuring results are comparable with experiences acquired under laboratory conditions (Rothfuss et al. 2015, Kühnhammer 2018, Quade et al. 2018) as well as field observations (Oerter & Bowen 2017, Gaj et al. 2016). Physical properties of the polypropylene tubing did not seem to alter during the course of the experiment and the tubes remained water-proof. Unstable measurements occurred mainly on days after the application of the rain pulses as well as during the morning hours. Short flushing phases of the tubes prior to the measurements enhanced stability without impacting isotopic composition. Morning measurements were mainly challenging on days when the temperature difference between day and night amounted to > 10 °C approximately. Then, measurements were conducted at a later point during the day. Apart from these days, predominantly higher air than soil temperatures favoured the diminution of condensation. Our soil measurements were therefore stable and reproducible. Nevertheless, condensation is a frequently addressed issue (Volkmann & Weiler 2014, Gaj et al. 2016, Oerter & Bowen 2017) and must always be considered when measuring at low temperatures or high temperature differences.

4.1.2 Measurement accuracy

Even under the unfavourable measurement conditions, with ambient air temperature amplitudes amounting up to 30 °C within 5 hour's time, mean accuracy of polypropylene tube measurements in medium standard vessels amounted to 0.29 ‰ deviation from the target value of δ^{18}O and 5.3 ‰ for δ^{2}H (see Figure A.2 in the Appendix). Nevertheless, real measurement accuracy cannot be determined in our experimental setup, since standards were explicitly measured to account for drift correction of the instrument due to fluctuating background conditions. Analytical performance of the water vapour probes was reported to be equivalent to laser analyzer accuracy under controlled conditions (Rothfuss et al. 2013).

In their *in situ* field study with the polypropylene probes, Oerter et al. (2017) did not find an altered value of spectral line width variable from CRDS in soil water vapour measurements in an agricultural field compared to silica-sand standard measurements. They observed an offset towards higher δ^{18}O vapour values in a soil with 9 % clay to be stronger at 5 % SWC than at 12 and 20 % SWC (Oerter et al. 2017). Hence, instead of applying Majoube's equation, they proposed corrections rather based on soil water and clay content to calculate liquid $\delta_{S\,liq}$ based on vapour $\delta_{S\,liq}$ values. Soil clay content from Freiburg Flugplatz experimental field site was determined to be 14 %. The processes of altered isotopic composition due to mineral water interaction could therefore affect our results (Gaj et al. 2017, Kühnhammer 2018). Measurements in sieved material from our study site in a recent laboratory experiment from Kühnhammer (2018) have shown polypropylene probes measurement accuracy to average ± 0.4 and ± 1.32 ‰ for δ^{18}O and δ^{2}H, respectively. Therefore, even though the real soil measurements in our experiment are expected to

more inaccuracy than in the standard vessels, the study of Kühnhammer (2018) indicates that in the results in sandy loam at our field site, lie still within the range of acceptable performance.

4.1.3 Soil water δ^2H and δ^{18}O dynamics

Repeated *in situ* sampling of several profiles over time showed that evaporation dynamics were measurable with the two shallow buried sampling probes even at field conditions. Relatively smaller linear regression slopes of pore water isotopic composition at preconditions compared to site-specific LMWL matches expectations based on Raleigh processes. After the application of a dual labelled depleted rain pulse, the pore water isotopic composition of all replicates notably drifted towards more negative values. Patterns from δ^{18}O signal were mirrored by deuterium. The fast temporal dynamics observed under field conditions are in line with findings from similar studies (Rothfuss et al. 2015, Oerter & Bowen 2017, Gaj et al. 2016, Piayda et al. 2017). High interception losses could be observed during the night after both labelling pulses due to high evaporative demand of the atmosphere. The first soil water vapour sample was analyzed 12 h after the rain events. Therefore, the isotopic signature of the incoming labelling pulse might be corrected for atmospheric water demand to obtain the isotopic signature of the water when it infiltrated the soil. The highest signal of rain pulse was always found at -3 cm and subsequently less depleted values were measured at each lower depth.

During drying, all δ values show a daily detectible drift towards the isotopic signature of the atmosphere. Changes of isotopic composition are hence not caused by drainage, but under the prevailing conditions, the driving force of soil water loss is evaporation. Observations of such evaporation fractionation down to -20 cm is in line with findings of numerous studies cited by Sprenger et al. (2016). Infiltration of water from the first labelling event was not visible from data in the soil water measurement probes. Isotopic composition revealed that a small fraction of the young water must have reached 40 cm depth. The isotopic signature was scarcely altered, compared to the changes in the shallow soil layers. Oerter & Bowen (2017) found similar results, after treating sandy loam with a pulse of labelled water, the corresponding isotopic signature could be found at depths above 20 cm only. Piayda et al. (2017) reported similar observations in a dry Mediterranean ecosystem with sandy soils where the fraction of young water strongly decreased in total water below 30 cm depth. Changes in soil water content were also not detectable in their case. Hence, they presumed replacement of old pre-event water by the new incoming precipitation pulse.

Distinct from the other soil horizons, in 40 cm depth, water content did not decline immediately after the precipitation pulse but rather stabilized at this depth. This indicates that small amounts of the water from the above lying horizons percolated further down to 40 cm depth. As we described above, a clay layer was found beneath this horizon, which indicates that water infiltration further down might have been decelerated. Moisture in this depth started declining stronger again after approximately six days, indicating that no further percolation occurred or the loss of water from this depth exceeded the gains. Small gradual changes in isotopic composition towards background conditions indicate that evaporation was reaching down to 40 cm. After the second rain event, isotopic water signature in 40 cm depth was altered substantially. The deeper penetration of water during this event is likely related to the higher amount of the applied water pulse.

Consequently, the distinct observations between the profiles at isotopic values of 3 cm depth might

be influenced by the heterogeneity of the topsoil relative gas diffusion coefficients. They control the speed of soil gases mixing with the atmosphere, and hence the advective removal of water vapour. Different plant vegetation patterns that shade surface and reduce temperature also imply reduced evaporation. This theory is supported by topsoil temperature measurements, varying over several degrees between the different profiles (see Figure A.1 in the Appendix).

Another anomaly, compared to the other replicates, was observed in profile 2. After the first labelling pulse on DoE 6, unexpectedly high values were found at 40 cm depth in profile 2. The values dropped rapidly on the following day and increased steadily from this moment onwards. The same partially non-sequential subsurface response was observed after the second labelling pulse, supporting the theory of an existing short-cut for water infiltration. The signals were both not as high as the incoming rain pulse and lower than the isotopic composition of the horizons above. A mixing of waters most likely must have occurred. The sudden decreases could indicate that we were observing a fast mobile fraction draining within one to three days, depending on the event intensity. The fading of the strikingly distinct isotopic signature, compared to measurements during the next days, might be related to lateral redistribution and mixing of water in the respective depth. Our theory that in this soil horizon lateral redistribution plays a role is supported by the sudden increases of soil water content in 40 cm depth in profiles 2 and 3 on DoE 22 after a naturally occuring rain event. Soil isotopic composition gives evidence for the intrusion of water from the surrounding field or a hole in the roof. Since none of the above lying θ probes, but all devices in 0.2 and 0.4 m depth detect increases in SWC, water flow must have mainly occurred laterally. The observations of material beneath 40 cm having higher clay content than the above lying horizons, and the former fluvial genesis of the soil support this conclusion. These observations highlight the valuable contribution of high temporal resolution measurements of soil water stable isotopes towards a better understanding of water-mixing processes within the soil.

Apart from the above mentioned observations, the spatial variability between the profiles was low. Point specific temporal information is lost, though, when averaged over all *in situ* observations in one specific depth.

4.2 Differences in water isotopic compositions between *in situ* and destructive sampling

4.2.1 Methodological differences associated with soil water isotope measurement

We found substantial differences between the results obtained from cryogenic vacuum extraction (CVE) analysis and *in situ* sampling probes. Differences were higher in upper soil horizons than at deeper soil layers and consistently lower signals of labelled water were found in CVE results. Nevertheless, an offset between linear regression lines of data from depths $\geq$ 40 cm in dual isotope space at natural conditions indicates systematic effects.

Measurement accuracy of the *in situ* method has been discussed in the section above. Accuracy of the cryogenic extraction on spiked replicates of dry soil from Freiburg Flugplatz field site was determined in a campaign during the previous year. Mean deviations from the target value were $0.7 \pm 0.2‰$ for $\delta^{18}O$ and $6.6 \pm 0.9‰$ for $\delta^{2}H$, respectively (Kübert 2017*a*). This is less precise than results from our repeated *in situ* standard measurements in sand and laboratory results with polypropylene tubings in the same soil as used in the spike tests.

In their review, Sprenger et al. (2015) compared different methods of pore water stable isotope

analysis and pointed out that, direct water vapour equilibrium method and CVE largely sample the same water pools, but with CVE also hygroscopic water can be extracted. The fraction of soil water sampled by different extraction methods is currently one of the main questions that the ecohydrological community is facing (Berry et al. 2018, Penna et al. 2018, Sprenger et al. 2018). Oerter & Bowen (2017) also observed differences between polypropylene probe measurements and vacuum extracted liquid water values to be systematical. In their study, the offset amounts only to around 5.8 ‰ in δ^2H. They concluded a physical separation of soil water pools occurring in their study system resulting from particle size. They built their assumption on the results from modelling and sand column experiments that found initial water content and particle sizes impacting how antecedent water is replaced by subsequent water infiltration events (Gouet-Kaplan et al. 2012). On the other hand, Volkmann & Weiler (2014) did not encounter such systematic offsets in the validation of their *in situ* water vapour equilibrium method under field conditions. In their review from 2016, Sprenger et al. show data from several studies which report a damping of an incoming precipitation signal in the soil profile. Furthermore, these studies noted a decreasing variability of soil water isotopes with depth independently from sampling strategies. They concluded that the damping is an effect of soil water mixing and that mixing occurs always to some degree, since all methods mark this dampening effect. Our results support both findings from these studies. We found effects of homogenization of the isotopic signal with both methods in 40 cm depth before and after the experiment.

In the very recently published experiment of Sprenger et al. (2018), using different methods to separate between fractions of soil water with different mobilities, they concluded that the relation between bulk soil and mobile soil water isotopic compositions was variable with time and no general offset dominated. Their explanation of the isotopic differences is related to the age of water in the different pore spaces. Our findings of an overall higher signal of labelling water measured with our field sampling method is additional evidence that each method may be sampling different fractions from each soil's field capacity. Hence, the direct comparability of the two methods is questionable.

Moving our considerations to a more practical point of view, the *in situ* sampling method showed to be facilitated at lower soil water contents. Destructive sampling in contrast was more labour intensive when soil was dry, due to the overall augmented penetration resistance of dry soil and high losses of sampling material. Additionally, lower SWC imposed problems during extraction analyses, when the portion of extracted water was too small to be analysed in the laser. Destructive sampling is afflicted with errors such as imprecise depth assignments, compaction of sampling material and kinetic fractionation due to evaporation of water from the sampled material at the atmosphere. The time required for *in situ* sampling in our experiment was approximately 40 minutes per sample, including flushing the system with dry air. Additionally, two entire days were needed for setup and dismantling work. Taking samples with soil cores, performing the vacuum extraction procedure and the measurement with CRDS afterwards lasted approximately 100 minutes per sample.

4.2.2 Transpiration related methodological differences

The results from plant transpiration measurements *in situ* and modelled values calculated with the equations of Craig and Gordon from cryogenic vacuum extraction analysis of bulk leaf water are only partly in agreement. During the first part of the experiment at field conditions, differences are within the range of sd indicating that comparability between modelled and observed values is given for at least a part of the experiment. Nevertheless, converse patterns of deuterium were observed during the second part of the experiment. Furthermore, field measurements showed to

be systematically higher depleted in both isotopologues.

In comparison with other extraction methods, Millar et al. (2018) observed results of CVE analysis also to be more depleted in δ^2H and δ^{18}O (Millar et al. 2018). They hypothesize plant leaves to contain water pools of different mobilities and CVE analysis to sample a mixtures of stable isotope signals connected to different uptake periods. This theory has already been proposed by other authors and is based on *in situ* field observations (referred to and measured by Simonin et al. (2013)). The increasing isotopic signature from DoE 25 in the results of the extraction analysis, could be explained by an overall increasing fraction of the event waters in all organic plant compounds. Similar to our findings from soil water vapour measurements, it is questionable, whether CVE can be taken as a baseline method for the evaluation of methods that map processes with higher temporal resolution.

Uncertainties are introduced when destructively sampling leaf material, instead of xylem, because transpiration isotopic composition must be modelled due to the evaporative enrichment in the leaves. In an unexceptional destructive approach, calculation the isotopic composition of evaporated water relies on approximations and not on actual measurements. Air temperature measurements in our study from 1.7 m above the canopy, for example, showed to have an offset of 1.2 °C relative to actual leaf temperatures measured *in situ*. The Craig and Gordon equation is also reported to not correctly approximate leaf physiological considerations, like leaf stomatal and boundary layer resistances, since the model originally was developed to describe fractionation above an open water surface (Craig & Gordon 1965, Gan et al. 2002, Dongmann et al. 1974, Yakir & Sternberg 2000). Craig and Gordon model results based on CVE analysis already have been reported to overestimate the observed isotopic depletion in (bulk) leaf water (Flanagan et al. 1991). This effect has been attributed by Gan et al. (2002), Farquhar et al. (2006), Simonin et al. (2013) to the isotopic gradients within the leaves, as a consequence of enrichment along the path of evaporation and the extraction of all liquid leaf content, including unfractionated vein water. This effect was reduced in our study by cutting out central veins of *C.jacea*. However, using the cuvette we only sampled from an area of 4 cm^2 instead of the whole leaf, as with the CVE method. A contribution of the isotopic heterogeneity at the leaf scale to the obtained discrepancies in our study cannot be excluded. Further, it has to be noted that we are comparing water isotopic composition of three replicates and several leaves per sample with one single observation *in situ*.

The *in situ* measurement method is a snapshot of the transpiration isotope signature from a specific moment in time. Transient conditions of environmental parameters related to leaf gas-exchange are affect isotopic composition of the transpiration water, since we are sampling from living plant material (Dubbert et al. 2017). Leaf cuvette measurements revealed that environmental condition changes at the leaf surface, for example photosynthetic active radiation, impacted photosynthesis rates, stomata conductance and transpiration activity during the experiment (see Figure A.8 in the Appendix). Leaf water at the evaporating sites is assumed to have reached isotopic steady state during midday. But the step changes in ambient conditions occur independently from daytime. These shifts in leaf transpiration rate showed to affect *rH* within the cuvette which impacted the isotopic composition of the water vapour instantly (Dubbert et al. 2017, Simonin et al. 2013). In these situations, water isotope measurements from cuvette cannot be assumed to reflect xylem water. Dubbert et al. (2017) observed offsets of 10 ‰ at step changes of *rH* from 60 to 30 %. In our study, the influence of isotopic composition is rather expected to amount to 1.3 ‰ (Dubbert, personal communication). Bulk leaf sampling to address questions of source water isotopic composition requires also steady-state conditions. Yet, results reflect an integrated signal

of the whole leaf and react rather within a timeframe of an hour to changes in environmental conditions (Farquhar et al. 2006). Therefore, bulk leaf sample measurements may be less afflicted of isotopic non-steady state than *in situ* measurements. Furthermore, analytical errors in bulk leaf measurements are assumed to be small. In an extraction method intercomparison, Millar et al. (2018) reported extraction analysis to yield leaf water extraction efficiencies from spring wheat samples of 99.8 % and deviation of analysis results to amount 1.02 and 2.81 ‰ ($\delta^{18}O$ and $\delta^{2}H$), respectively. No correction for instrument measurement drift was applied to *in situ* transpiration measurements.

Nevertheless, when supervised continuous measurements *in situ* are supervised and can be directly adapted. Additionally, with all measured variables at the leaf level non-steady conditions can be more easily identified and then excluded from the measurements. This is not the case for destructively sampled material, where sampling and analysis can be far apart in time, which makes the traceability of potential disturbed transpiratory flow balances in the leaf more difficult or impossible.

4.3 Impact of distinct methods on root water uptake modelling

The different model input distributions based on mean daily measurements of two methods and their sd yielded different results. Although they all suggest high fractions of water uptake from soil depths beneath 5 cm, temporal variation is high.

The model structure is designed to assume equal volumes of contribution from all sources if the parameter "concentration effect" is not defined (Parnell et al. 2010, Phillips & Gregg 2003). This explains uptake probability distributions suggesting equal contributions of all horizons to the isotopic signature of plant transpiration water. This result indicates that under pre-conditions, differences between the horizons are too little or variance is too high to distinguish between the possible sources. The application of the labelled water pulse on DoE 6 enabled sufficient information for the model to distinguish between the different sources, despite spatial variability and non-parametric statistical results.

In our experiment, both models suggest that even after heavy rain events and high water availability in the topsoil, *Centauera jacea* remains using a higher fraction of water from deeper soil horizons. Model results based on the cryogenic extraction method show the temporal response of *C. jacea* to last 4 to 5 days after the first rain event occurred, until the uptake from more shallow soil was increased substantially. *In situ* measurements show overall little variation in the uptake from topsoil. Soil water measurements in our study showed water content in the topsoil to have the highest variability, whereas in 40 cm depth, water seemed to be declining only slowly. This might explain the high fraction of water use by *C. jacea* from this horizon. Slower reaction to incoming precipitation pulses might be a result of the need to reactivate topsoil roots to prevent loss of water due to lower potential of soil matrix in topsoil during dry periods (Volkmann et al. 2016) and hence an adaptation to dominant soil moisture distribution at the site. Piayda et al. (2017) also showed in a mediterranean system with a herbaceous layer of annual plants that root water uptake depth did not considerably changed after applying a rain impulse. Plants were only shifting their uptake during the first two days after the rain pulse, but then continuing to use mainly water from 30 cm depth. They concluded that lower but more resilient production could be achieved by the plants by limiting rooting depth and water uptake into subsoil (Piayda et al. 2017). Our results match their observations, confirming the applicability of the *in situ* method.

Observations and RWU modelling of a *C. jacea* in a soil column laboratory experiment from Kühnhammer (2018) revealed a preference of the plant's water uptake from soil compartments where water was least tightly bound. As a reaction to an incoming precipitation pulse, the plant water uptake was shifted towards more shallow soil depths within less than a day (Kühnhammer 2018). These results let them conclude that drought adapted species could have the strategy to use as much water of incoming rain events as possible, before it percolates deeper into the soil or evaporates from the surface. The laboratory experiment provides valuable information about the physiological characteristics of the species. An explanation for differences between observations of reactions from C. jacea under field conditions might be that the plant individuals were older than the ones used in the soil column experiment (Kühnhammer, personal communication). In our experiment first individuals of C. jacea on the plot started flowering on DoE 22. This indicates that in our experiment the individuals were in a completely different state of their life cycle than the plant in the soil column.

Regarding *Arrhenaterum elatius*, the model results suggest two completely different plant strategies that can both be explained. Modelling results based on *in situ* measurements suggest a similar plant strategy as *C. jacea*, with main water use from 40 cm depth. Water uptake in the uppermost cm mostly occurs after rain events but the fractions of topsoil water use did not exceed 20 % and decreases subsequently when the uppermost centimeters were drying. In contrast, the water uptake pattern of *A. elatius* based on results from destructive sampling indicates water from the upper 5 cm to cover up to >60 % of total transpiration during days after heavy precipitation. The share of water from depths beneath 20 cm under dry conditions accounts for 60 %. Shallow roots likely react within a day, but after the second rain event, the grasses probably maintained to draw an overall higher fraction of water from deeper horizons.

Schwinning et al. (2002) observed the water uptake depth of the perennial grass species *Hilaria jamesii* to be only augmented in spring, whereas in summer, the rates of water uptake from the grass in shallow soil were not distinguishable from shrubs. They also observed a smaller reaction of the plant community's proportion of shallow soil water uptake in summer to an irrigation event during their experiment. Grasses at drought-affected plots in a study in Switzerland conducted by Prechsl et al. (2015) showed that under similar soil moisture conditions, contribution of water from 20 cm depth to isotopic composition of plant transpiration was always higher on drought affected plots. Again, this fits better to the model results from *in situ* measurements.

Temporal variations of the uptake patterns highlight the questionability of one-day measurement campaigns at different seasons as conducted in other experiments (Prechsl et al. 2015, Bachmann et al. 2015). This is especially visible in the temporal inconsistency of the results from destructively obtained samples of *C. jacea* before application of the second labelling pulse. A higher spatial *in situ* sampling frequency between -5 and -10 cm in this study might have been useful since contribution to root water uptake from these depths is likely due to the high root density. Water retention curves obtained from soil cores in these depths showed that soil hydraulic properties are favourable for plant water uptake (Dahlmann 2018) (see Figure A.7). Nevertheless, even though SIAR enables the inclusion of an assessment of the consequence of input uncertainties, it is solely based on statistical assumptions. The usefulness of input information for the model results depends on how narrow the contribution ranges of the sources are (Phillips & Gregg 2003). For the *in situ* measured input data, we averaged over space, broadening the ranges of the possible input variables and reducing the temporal information content. Another option would be to use the different profiles and their isotopic distribution as sources for different models and to average over the obtained probability

distributions to observe whether temporal changes in modelled source shares yield clearer results. Including leaf water potential and water retention curve to restrict model sources could also improve model performance, since it would not only introduce more bio-physical considerations but also enhance empirical robustness due to reduction of sources (Parnell et al. 2010, Phillips & Gregg 2003).

Due to leaf cuvette measurements and the determination of soil physical characteristics in the laboratory, further analysis of the data collected could help to parameterize more sophisticated model approaches to understand the temporal and species-specific dynamics of root water uptake. In the context of this work, however, a further evaluation of the data was too extensive.

4.4 Methodological and technical limitations of the *in situ* technique

One of the main interests for *in situ* sampling is the demand for non-destructive sampling methods. There are several main critical examinations of the herein tested sampling method that need to be discussed in this regard.

One critical point is the installation of the sampling probe in the field. Every excavation and refilling of soil alter structures of natural soil genesis, especially in highly heterogeneous soils with horizons from fluvial depositions that can combine high vertical with low lateral variability, due to ancient flow dynamics. We observed a systematic offset of the isotopic composition of samples drawn with a soil corer between the refilled and undisturbed soil material. This result indicates that the altered soil stratification had an impact on water infiltration and/or gas exchange processes between the soil and the atmosphere. Higher porosities, for example, could have led to faster infiltration as well as augmented diffusional transport of soil air. Since we have only a single comparison value per depth a quantification and correction for this systematic offset was not possible. Hence, it is questionable, if the chosen methodological approach for the method comparison was reasonable. One of the few *in situ* sampling probe field experiments from Oerter et al. (2017), for example, was conducted at a field site of managed soil, "without distinctive signs of pedogenic development". Even though they also reported mean systematic offsets of 8.05 ‰ (δ^2H) and -3.9 ‰ (δ^{18}O) between results from CVE and *in situ* sampling probes, they did not report to have tested for differences in CVE results of undisturbed and disturbed material in their experimental setup. Their explanation was mainly related to the question of potential differences between the sampled water pools by each method, which has already been discussed in more detail in section 4.1.3. However, this problem is more likely to be seen as a problem of installing the probes in the soil and does not question the reliability of the method. Advanced development of the probe design could reduce the impacts.

A second critical question would be whether an alteration of water content and kinetic fractionation effect occurs by the export of depleted water vapour during each sampling. Dry air as a transport medium hereby does not replace the extracted amount of water. The question arises, under which conditions sampling will have significant influence on isotopic equilibrium and water content in the sampled pore space. Yet, measurements of pore water vapour isotopic composition by Rothfuss et al. (2013) showed that even sampling over long time periods and high flow rates did not have an impact on isotopic composition of water vapour. They reported obtained calibration relationships under laboratory conditions to be only a function of temperature. These findings are supported by *in situ* measurements from soil probes used by Volkmann & Weiler (2014) indicating that chemical equilibrium of liquid-vapour system remained stable under the applied conditions. During our

experiment, we could not detect an enrichment of standard soil isotopic composition over time. Our standard vessels may not be sufficiently representative, because they contained a higher soil water content compared to the field resulting in a lower relative share of withdrawn water per sample from total water content. It should be further investigated under which soil conditions sampling procedure and timeframe the method is altering soil water isotopic composition to a degree that results are not reflecting natural processes anymore but rather the impact of the sampling method.

In a recent study, Lin et al. (2018) found equilibrium isotopic fractionation factors to be different in soil pore water and its water vapour than for liquid and vapour of bulk water. The effect is predicted to be strongest at low water contents. Continued efforts should be directed towards advancements of the physical models that the soil water isotope data processing relies on.

The velocity of naturally occurring soil gas transport should also be taken into consideration. Measurement of concentrations, assuming transport of soil water vapour to be constant in time or sufficiently small to play a minor role in the results is questionable. Especially in uppermost soil layers, these effects are likely to significantly alter isotopic equilibrium. The fraction of the measured value that diffuses into the membrane tube from air-filled pores, and does not evaporates from a waterfilled pore directly into the membrane tube must be considered rather as a sampling point from a steady gradient; namely, the gradient of soil air isotopic composition driven by water vapour partial pressure differences between soil and atmosphere. Then, the sample is only partly reflecting the isotopic composition of water vapour from the exact sampling depth where the specific probe is installed. With a rising percentage of air-filled pore space, this proportion grows (Vanderborght et al. 2017). In our study, it amounts to at least between 70 and 90 % of all pores. Therefore, the effect of soil gas fluxes on the sampling method should be further evaluated. Furthermore, the vapour probe could influence flow dynamics within the soil. A laterally staggered arrangement of soil vapour sampling tubes, as considered in the setup of Oerter & Bowen (2017), would have been more favourable to prevent influence of overlying probes on vertical water flow.

Limitations of the unattended application in the field are similar to the restrictions of the in-situ measuring system developed by Volkmann & Weiler (2014). Prerequirement of all *in situ* monitoring of water stable isotopes in the field is a sufficient power supply for the CRDS instrument. Dry gas supply must also be organized and standard vessels must contain sufficient volumes of water for the number of samples that are drawn over the course of the experiment. To impede condensation effects, a flushing routine must be established and checked regularly to be adapted based on the actual requirements. Another option, inevitable for measurements during winter or at cold temperatures, is a temperature control system (heating) like in the setup of Oerter & Bowen (2017).

5 Conclusion and Outlook

In this study, we successfully tested a non-destructive monitoring technique for soil water isotopic composition under field conditions. Dynamics of evaporation, infiltration and mixing of water in the soil could be traced on a daily resolution. The comparison between different replicates enabled us to distinguish temporal processes from spatial heterogeneity. Measurements under field conditions were stable and condensation did not occur as long as air temperature was higher than subsoil temperature. We find that depending on precipitation intensity, incoming precipitation pulses only rewetted topsoil or infiltrated to 40 cm depth. The highest fractions of the precipitation pulse were found in the topsoil, but changes in isotopic signatures of all depths indicate deeper percolation to occur at least after the heavier of the two rain events. The labelling approach helped us to distinguish between different soil depths.

Furthermore, with the combination of *in situ* transpiration measurements, we could link the coupled short-term dynamics of rainwater in the soil to the uptake responses of two grassland species. The plant transpiration water was isotopically not distinct from soil water and reflected a mixture of water from sampled depths. Modeled rwu fractions based on *in situ* measurements showed better temporal consistency than results obtained by destructive sampling. They could be logically interpreted and were in agreement with findings from former studies on reactions of grassland species on water uptake after drought. In comparison with results from cryogenic extraction analyses, we found systematic offsets. These offsets in soil δ^2H and δ^{18}O have already been addressed by other authors and might be related to processes of water isotopic mixing occurring at different timescales. Modelling isotopic composition of transpiration water from bulk leaf samples mostly did not meet observations in the field, yielding in physiologically unrealistic rwu fractions for some days during the experiment.

Confirming experiences of Volkmann et al. (2016) and Oerter & Bowen (2017), we also evaluated the ability to measure repeatedly at identical locations in the field to enable us to ascribe observations to processes. Therefore, we strongly recommend reinforced use of non-destructive monitoring techniques under field conditions for plant and soil measurements for investigations of rwu.

More certainty must be gained about the fraction of water obtained by the different methods: this concerns the total water content of the soil as well as water contained in plant tissues. Based on the theory that vacuum extraction samples reflect an integrated signal of the isotopic composition of soil water, including pores with delayed mixing time, further analyses to differentiate between the fast and the slow reacting domains and distributions of soil water residence times must be conducted. As proposed by Oerter & Bowen (2017), and tested recently within a different methodical approach by Sprenger et al. (2018), *in situ* monitoring of δ^2H and δ^{18}O combined with vacuum extraction methods could give valuable insights on processes on different temporal scales. Temporal resolutions of processes relevant for each research question should be considered to choose adequate sampling method in studies using stable isotope analysis. Combining experiences from the different scientific communities of pedology, hydrology, plant physiology and atmospheric sciences can help to prevent sources of uncertainty and pave the way to rapidly resolve remaining knowledge gaps.

References

Alduchov, O. A. & Eskridge, R. E. (1996), 'Improved Magnus Form Approximation of Saturation Vapor Pressure.', *Journal of Applied Meteorology* **35**, 601–609.

Bachmann, D., Gockele, A., Ravenek, J. M., Roscher, C., Strecker, T., Weigelt, A. & Buchmann, N. (2015), 'No evidence of complementary water use along a plant species richness gradient in temperate experimental grasslands', *PLoS ONE* **10**(1), 1–14.

Berry, Z. C., Evaristo, J., Moore, G., Poca, M., Steppe, K., Verrot, L., Asbjornsen, H., Borma, L. S., Bretfeld, M., Hervé-Fernández, P., Seyfried, M., Schwendenmann, L., Sinacore, K., De Wispelaere, L. & McDonnell, J. (2018), 'The two water worlds hypothesis: Addressing multiple working hypotheses and proposing a way forward', *Ecohydrology* **11**(3), 1–10.

Craig, H. & Gordon, L. I. (1965), 'Deuterium and oxygen 18 variations in the ocean and the marine atmosphere'.

Dahlmann, A. (2018), 'Vergleich zweier Methoden zur Bestimmung der Isotopensignatur von Boden- und Pflanzenwasser unter Berücksichtigung verschiedener Umweltparameter'. Bachelor's Thesis, Albert-Ludwigs University Freiburg, Germany.

Dongmann, G., Nürnberg, H. W., Förstel, H. & Wagener, K. (1974), 'On the enrichment of $H_2{}^{18}O$ in the leaves of transpiring plants', *Radiation and Environmental Biophysics* **11**(1), 41–52.

Dubbert, M., Cuntz, M., Piayda, A., Maguás, C. & Werner, C. (2013), 'Partitioning evapotranspiration - Testing the Craig and Gordon model with field measurements of oxygen isotope ratios of evaporative fluxes', *Journal of Hydrology* **496**, 142–153.

Dubbert, M., Kübert, A. & Werner, C. (2017), 'Impact of Leaf Traits on Temporal Dynamics of Transpired Oxygen Isotope Signatures and Its Impact on Atmospheric Vapor', *Frontiers in Plant Science* **8**(January), 1–12.

Dubbert, M., Piayda, A., Cuntz, M., Correia, A. C., Costa e Silva, F., Pereira, J. S. & Werner, C. (2014), 'Stable oxygen isotope and flux partitioning demonstrates understory of an oak savanna contributes up to half of ecosystem carbon and water exchange', *Frontiers in Plant Science* **5**(October), 1–16.

Dubbert, M., Piayda, A., Cuntz, M. & Werner, C. (2014), 'Oxygen isotope signatures of transpired water vapor – the role of isotopic non-steady-state transpiration of Mediterranean cork-oaks (Quercus suber L .) under natural conditions', *New Phytologist* **16**, 2014.

Dubbert, M. & Werner, C. (2018), 'Water fluxes mediated by vegetation: emerging isotopic insights at the soil and atmosphere interfaces', *New Phytologist* pp. 0–2.

DWD, D. W. D. (n.d.), 'DWD online lexicon'.

DWD Climate Data Center: Daily climate observations Germany (2018), \/climate/daily/kl/}.

Ehleringer, J. R. & Dawson, T. E. (1992), 'Water uptake by plants: perspectives from stable isotope', *Plant, Cell & Environment* **15**, 1073–1082.

Evaristo, J., McDonnell, J. J. & Clemens, J. (2017), 'Plant source water apportionment using stable isotopes: A comparison of simple linear, two-compartment mixing model approaches', *Hydrological Processes* **31**(21), 3750–3758.

Farquhar, G. D. & Cernusak, L. A. (2005), 'On the isotopic composition of leaf water in the non-steady state', *Functional Plant Biology* **32**(1974), 293–303.

Farquhar, G. D., Cernusak, L. A. & Barnes, B. (2006), 'Heavy Water Fractionation during Transpiration', *Plant Physiology* **143**(1), 11–18.

Flanagan, L. B., Bain, J. F. & Ehleringer, J. R. (1991), 'Stable oxygen and hydrogen isotope composition of leaf water in C3 and C4 plant species under field conditions', *Oecologia* **88**, 394–400.

Flechard, C. R., Neftel, A., Jocher, M., Ammann, C., Leifeld, J. & Fuhrer, J. (2007), 'Temporal changes in soil pore space CO_2 concentration and storage under permanent grassland', *Agricultural and Forest Meteorology* **142**(1), 66–84.

Gaj, M., Beyer, M., Koeniger, P., Wanke, H., Hamutoko, J. & Himmelsbach, T. (2016), 'In situ unsaturated zone water stable isotope (2H and 18O) measurements in semi-arid environments: A soil water balance', *Hydrology and Earth System Sciences* **20**(2), 715–731.

Gaj, M., Kaufhold, S., Koeniger, P., Beyer, M., Weiler, M. & Himmelsbach, T. (2017), 'Mineral mediated isotope fractionation of soil water', *Rapid Communications in Mass Spectrometry* **31**(3), 269–280.

Gan, K. S., Wong, S. C., Yong Hong, J. W. & Farquhar, G. D. (2002), '18o spatial patterns of vein xylem water, leaf water, and dry matter in cotton leaves', *Plant Physiology* **130**(October 2002), 1008–1021.

Gonfiantini, R. (1978), 'Standards for stable isotope measurements in natural compounds', *Nature* **271**(5645), 534.

Gouet-Kaplan, M., Arye, G. & Berkowitz, B. (2012), 'Interplay between resident and infiltrating water: Estimates from transient water flow and solute transport', *Journal of Hydrology* **458-459**, 40–50.

Gralher, B., Herbstritt, B., Weiler, M., Wassenaar, L. I. & Stumpp, C. (2016), 'Correcting Laser-Based Water Stable Isotope Readings Biased by Carrier Gas Changes', *Environmental Science and Technology* **50**(13), 7074–7081.

Gut, A., Blatter, A., Fahrni, M., Lehmann, B. E., Neftel, A. & Staffelbach, T. (1998), 'A new membrane tube technique (METT) for continuous gas measurements in soils', *Education* pp. 79–88.

Kulmatiski, A. & Beard, K. H. (2013), 'Root niche partitioning among grasses, saplings, and trees measured using a tracer technique', *Oecologia* **171**(1), 25–37.

Kübert, A. (2017*a*), 'Cryogenic vacuum extraction spike test with soil from experimental fieldsite freiburg flugplatz'. unpublished raw data.

Kübert, A. (2017*b*), 'Precipitation isotopic composition at experimental fieldsite freiburg flugplatz'. unpublished raw data.

Kühnhammer, K. (2018), 'Monitoring root water uptake of centaurea jacea using water stable isotopes'. Master's Thesis, Albert-Ludwigs University Freiburg, Germany.

Lin, Y., Horita, J. & Abe, O. (2018), 'Adsorption isotope effects of water on mesoporous silica and alumina with implications for the land-vegetation-atmosphere system', *Geochimica et Cosmochimica Acta* **223**(September), 520–536.

Majoube, M. (1971), 'Fractionation in O-18 between ice and water vapor', *Journal de Chimie Physique et de Physico-Chimie Biologique* **68**(4), 625–+.

Merlivat, L. (1978), 'Molecular diffusivities of H 2 16 O, HD 16 O, and H 2 18 O in gases', *The Journal of Chemical Physics* **69**(6), 2864–2871.

Millar, C., Pratt, D., Schneider, D. J. & McDonnell, J. J. (2018), 'A comparison of extraction systems for plant water stable isotope analysis', *Rapid Communications in Mass Spectrometry* **32**(13), 1031–1044.

Oerter, E. J. & Bowen, G. (2017), 'In situ monitoring of H and O stable isotopes in soil water reveals ecohydrologic dynamics in managed soil systems', *Ecohydrology* **10**(4), 1–13.

Oerter, E. J., Perelet, A., Pardyjak, E. & Bowen, G. (2017), 'Membrane inlet laser spectroscopy to measure H and O stable isotope compositions of soil and sediment pore water with high sample throughput', *Rapid Communications in Mass Spectrometry* **31**, 75–84.

Orlowski, N., Breuer, L., Nicolas, A., Boeckx, P., Brumbt, C., Cook, C., Dubbert, M., Dyckmans, J., Gallagher, B., Gralher, B., Herbstritt, B., Hervé-Fernández, P., Hissler, C., Koeniger, P., Legout, A., Joan Macdonald, C., Oyarzun, C., Redelstein, R., Seidler, C. & Mcdonnell, J. (2018), 'Inter-laboratory comparison of cryogenic water extraction systems for stable isotope analysis of soil water', *Hydrology and Earth System Sciences Discussions* pp. 1–36.

Orlowski, N., Frede, H.-G., Brüggemann, N. & Breuer, L. (2013), 'Validation and application of a cryogenic vacuum extraction system for soil and plant water extraction for isotope analysis', *Journal of Sensors and Sensor Systems* **2**, 179–193.

Orlowski, N., Pratt, D. L. & McDonnell, J. J. (2016), 'Intercomparison of soil pore water extraction methods for stable isotope analysis', *Hydrological Processes* **30**(19), 3434–3449.

Parent, F., Plain, C., Epron, D., Maier, M. & Longdoz, B. (2013), 'A new method for continuously measuring the δ13C of soil CO2concentrations at different depths by laser spectrometry', *European Journal of Soil Science* **64**(4), 516–525.

Parnell, A. C., Inger, R., Bearhop, S. & Jackson, A. L. (2010), 'Source Partitioning Using Stable Isotopes: Coping with Too Much Variation', *PLoS ONE* **5**(3), e9672.

Parnell, A. & Jackson, A. (2013), *siar: Stable Isotope Analysis in R*. R package version 4.2.
URL: *https://CRAN.R-project.org/package=siar*

Penna, D., Hopp, L., Scandellari, F., Allen, S. T., Benettin, P., Beyer, M. & Geris, J. (2018), 'Ideas and perspectives : Tracing terrestrial ecosystem water fluxes using hydrogen and oxygen stable isotopes – challenges and opportunities from an interdisciplinary perspective', *Biogeosciences* **15**(October), 6399–6415.

Penna, D., Stenni, B., Sanda, M., Wrede, S., Bogaard, T. A., Michelini, M., Fischer, B. M. C., Gobbi, A., Mantese, N., Zuecco, G., Borga, M., Bonazza, M., Sobotková, M., Čejková, B. & Wassenaar, L. I. (2012), 'Technical note: Evaluation of between-sample memory effects in the analysis of δ2H and δ18O of water samples measured by laser spectroscopes', *Hydrology and Earth System Sciences* **16**(10), 3925–3933.

Phillips, D. L. & Gregg, J. W. (2003), 'Source partitioning using stable isotopes: Coping with too many sources', *Oecologia* **136**(2), 261–269.

Piayda, A., Dubbert, M., Siegwolf, R., Cuntz, M. & Werner, C. (2017), 'Quantification of dynamic soil-vegetation feedbacks following an isotopically labelled precipitation pulse', *Biogeosciences* **14**(9), 2293–2306.

Prechsl, U. E., Burri, S., Gilgen, A. K., Kahmen, A. & Buchmann, N. (2015), 'No shift to a deeper water uptake depth in response to summer drought of two lowland and sub-alpine C3-grasslands in Switzerland', *Oecologia* **177**(1), 97–111.

Quade, M., Brüggemann, N., Graf, A., Vanderborght, J., Vereecken, H. & Rothfuss, Y. (2018), 'Investigation of Kinetic Isotopic Fractionation of Water During Bare Soil Evaporation', *Water Resources Research* **54**(9), 6909–6928.

R Core Team (2017), 'R: A language and environment for statistical computing'.
URL: *https:// www.R-project.org/*

Rothfuss, Y. & Javaux, M. (2017), 'Reviews and syntheses: Isotopic approaches to quantify root water uptake: A review and comparison of methods', *Biogeosciences* **14**(8), 2199–2224.

Rothfuss, Y., Merz, S., Vanderborght, J., Hermes, N., Weuthen, A., Pohlmeier, A., Vereecken, H. & Brüggemann, N. (2015), 'Long-term and high-frequency non-destructive monitoring of water stable isotope profiles in an evaporating soil column', *Hydrology and Earth System Sciences* **19**(10), 4067–4080.

Rothfuss, Y., Vereecken, H. & Brüggemann, N. (2013), 'Monitoring water stable isotopic composition in soils using gas-permeable tubing and infrared laser absorption spectroscopy', *Water Resources Research* **49**(6), 3747–3755.

Schmidt, M., Maseyk, K., Lett, C., Biron, P., Richard, P., Bariac, T. & Seibt, U. (2010), 'Concentration effects on laser-based d18O and d2H measurements and implications for the calibration of vapour measurements with liquid standards', *Rapid Communications in Mass Spectrometry* **24**(16), 3553–3561.

Schwinning, S., Davis, K., Richardson, L. & Ehleringer, J. R. (2002), 'Deuterium enriched irrigation indicates different forms of rain use in shrub/grass species of the Colorado Plateau', *Oecologia* **130**(3), 345–355.

Schymanski, S. J., Sivapalan, M., Roderick, M. L., Beringer, J. & Hutley, L. B. (2008), 'An optimality-based model of the coupled soil moisture and root dynamics', pp. 913–932.

Seeger, S. & Weiler, M. (2016), Optimizing plant water uptake source depths estimation by stable water isotope labeling.

Simonin, K. A., Roddy, A. B., Link, P., Apodaca, R., Tu, K. P., Hu, J., Dawson, T. E. & Barbour, M. M. (2013), 'Isotopic composition of transpiration and rates of change in leaf water isotopologue storage in response to environmental variables', *Plant, Cell and Environment* **36**(12), 2190–2206.

Solomon, S., Qin, D., Manning, M., Averyt, K. & Marquis, M. (2007), *Climate change 2007-the physical science basis: Working group I contribution to the fourth assessment report of the IPCC*, Vol. 4, Cambridge university press.

Sprenger, M., Herbstritt, B. & Weiler, M. (2015), 'Established methods and new opportunities for pore water stable isotope analysis', **5192**(September), 5174–5192.

Sprenger, M., Leistert, H., Gimbel, K. & Weiler, M. (2016), 'Illuminating hydrological processes at the soil-vegetation-atmosphere interface with water stable isotopes', *Reviews of Geophysics* **54**(section 6), 119–161.

Sprenger, M., Tetzlaff, D., Buttle, J., Laudon, H., Leistert, H., Mitchell, C. P., Snelgrove, J., Weiler, M. & Soulsby, C. (2018), 'Measuring and Modeling Stable Isotopes of Mobile and Bulk Soil Water', *Vadose Zone Journal* **17**(1), 0.

Stumpp, C., Brüggemann, N. & Wingate, L. (2018), 'Stable Isotope Approaches in Vadose Zone Research', *Vadose Zone Journal* **17**(1), 0.

Van Geldern, R. & Barth, J. A. C. (2012), 'Optimization of instrument setup and post-run corrections for oxygen and hydrogen stable isotope measurements of water by isotope ratio infrared spectroscopy (IRIS)', *Limnology and Oceanography: Methods* **10**(DECEMBER), 1024–1036.

Vanderborght, J., Fetzer, T., Mosthaf, K., Smits, K. M. & Helmig, R. (2017), 'Heat and water transport in soils and across the soil-atmosphere interface: 1. Theory and different model concepts', *Water Resources Research* **53**(2), 1057–1079.

Volkmann, T. H., Haberer, K., Gessler, A. & Weiler, M. (2016), 'High-resolution isotope measurements resolve rapid ecohydrological dynamics at the soil-plant interface', *New Phytologist* **210**(3), 839–849.

Volkmann, T. H. M. & Weiler, M. (2014), 'Continual in situ monitoring of pore water stable isotopes in the subsurface', *Hydrology and Earth System Sciences* **18**(5), 1819–1833.

Wang, L., Good, S. P., Caylor, K. K. & Cernusak, L. A. (2012), 'Direct quantification of leaf transpiration isotopic composition', *Agricultural and Forest Meteorology* **154-155**, 127–135.

Werner, C., Schnyder, H., Cuntz, M., Keitel, C., Zeeman, M. J., Dawson, T. E., Badeck, F. W., Brugnoli, E., Ghashghaie, J., Grams, T. E., Kayler, Z. E., Lakatos, M., Lee, X., Máguas, C., Ogée, J., Rascher, K. G., Siegwolf, R. T., Unger, S., Welker, J., Wingate, L. & Gessler, A. (2012), 'Progress and challenges in using stable isotopes to trace plant carbon and water relations across scales', *Biogeosciences* **9**(8), 3083–3111.

Yakir, D. & Sternberg, L. D. S. L. (2000), 'The use of stable isotopes to study ecosystem gas exchange', *Oecologia* **123**(3), 297–311.

Declaration of Authorship

I hereby declare and confirm that this thesis is entirely the result of my own original work. Where other sources of information have been used, they have been indicated as such and properly acknowledged.
I further declare that this or similar work has not been submitted for credit elsewhere.

Place, date

Signature

Appendix

A1 List of Symbols

Symbol	Description	Unit
α_k	Kinetic fractionation factor	
α^+	Equilibrium fractionation factor	
CO_2	Carbon dioxide	
Δ	Difference operator	
$\delta^{18}O$	Oxygen stable isotope signature	‰
δ^2H	Hydrogen stable isotope signature (Deuterium)	‰
h	Relative humidity normalized to leaf temperature	%
H	Hydrogen	
O	Oxygen	
PAR	Photosynthetically active radiation	µE * $m^{-2}s^{-1}$
T	Temperature	°C or K
rH	Relative air humidity	%
θ	Volumetric soil water content	m^3m^{-3}
vpd	Water vapour pressure deficit	hPa
wvmr	Water vapour mixing ratio	ppmv

Subscript	Description
ATM	Atmosphere
gas	Water vapour
liq	Liquid water
S	Soil
T	Transpiration

A2 List of Abbreviations

Abbreviation	Description
BIMM	Bayesian isotope mixing modeling
CEST	Central European Summer Time
CJ	*Centaurea jacea*
CRDS	Cavity Ring-Down Spectroscopy
CVE	Cryogenic vacuum extraction
DoE	Day of experiment
GMWL	Global Meteoric Water Line
IAEA	International Atomic Energy Agency
IRIS	Isotope Ratio Infrared Spectroscopy
LMWL	Local Meteoric Water Line
LRS	Linear regression slope
mfv	Most frequent value
POA	*Arrhenatherum elatius*
PP	Liquid Precipitation
$STD_{H,M,L}$	Working Standard, subscript denoting heavy, medium and light
sd	Standard deviation
RWU	Root water uptake
SWC	Soil Water Content

A3 Temperature and soil water content over time in the different profiles

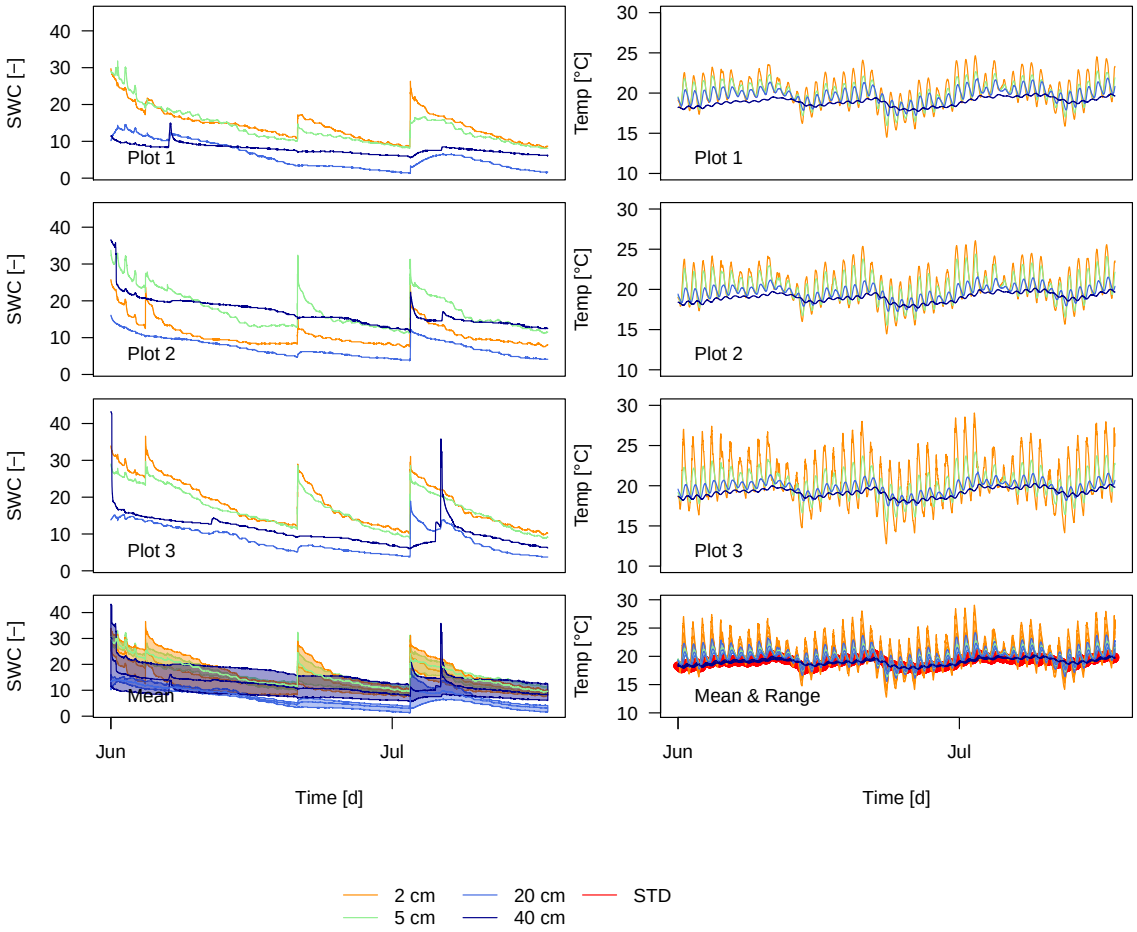

Figure A.1: Volumetric soil water content and temperature measurements for (a,e) profile 1 (b,f) profile 2 (c,g) profile 3. Panels (d) and (h) show mean and ranges of all profiles as well as well as soil temperature around buried standard vessels.

A4 Field standard measurement accuracy and precision

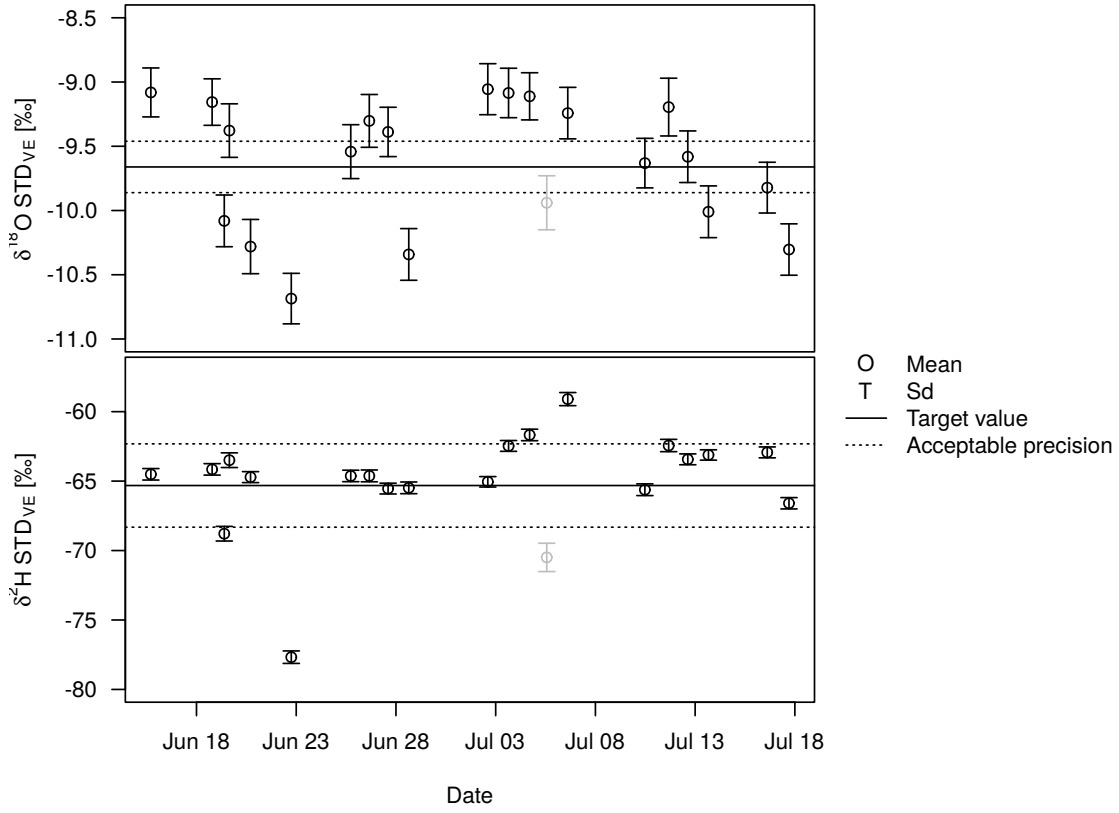

Figure A.2: Measurement precision of field STD_M over time. Solid black line and vertical lines are marking target value and usual measurement precision. Values in grey show deviation from mean measured value of >0.3 and >1 for $\delta^{18}O$ and $\delta^{2}H$, respectively, were considered untrustworthy and excluded. Due to y-axis scale, only one of three excluded values are shown.

A5 Relationship between volumetric water content and standard measurement precision

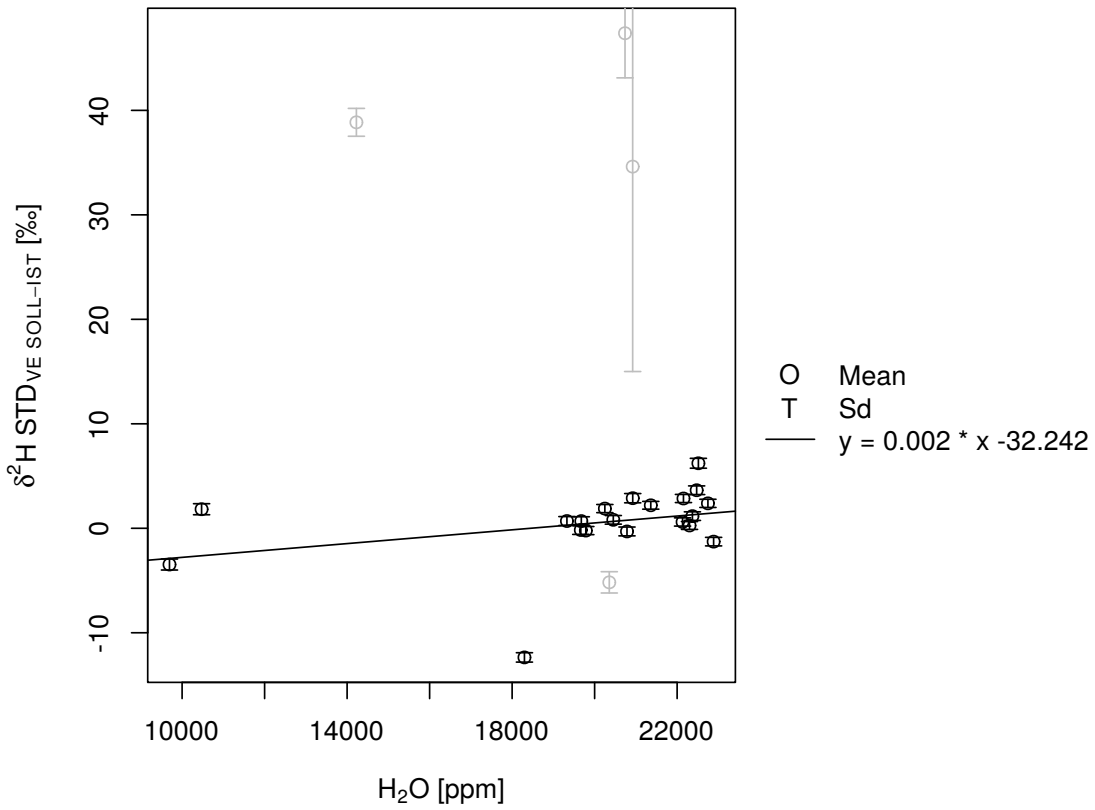

Figure A.3: Relationship between measurement precision of field STD_M and water vapour mixing ratios. Values in grey show deviation from mean measured value of >0.3 and >1 for $\delta^{18}O$ and $\delta^{2}H$, respectively, were considered untrustworthy and excluded.

A6 Standards autosampler measurements

During laboratory measurements, cryogenic extracted samples were mixed with samples from centrifugation analysis. In the subsequent measurement period we observed high organic contamination in CRDS, that could not be appropriately corrected by the calibration and standardization procedure proposed by Van Geldern & Barth (2012). Millar et al. (2018) were reporting similar problems. Additionally, CRDS application settings of employed carrier gas got changed under repair, resulting in a shift of isotope readings. We observed shifts similar to the conducted investigations by Gralher et al. (2016) but applied conventional calibration was adequate to postcorrect the emerging offset.

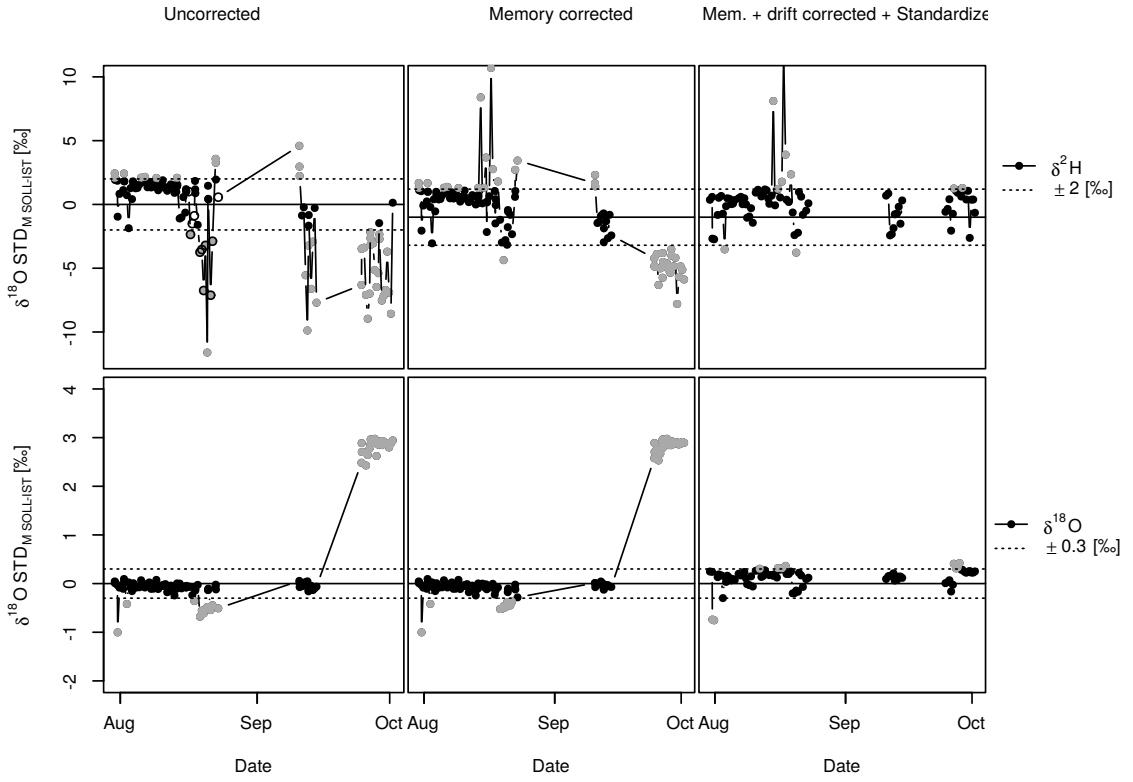

Figure A.4: Raw measurements and effect of each correction step applying method proposed by Van Geldern & Barth (2012) on STD_{medium} from measurement of liquid sample material over time. Upper row panels show STD_{medium} δ^2H lower row panels $\delta^{18}O$ deviation from true value. Mostright panels show corrected STD_{medium} values. Black values are within the ranges of acceptable performance reported in the literature (Orlowski et al. 2016, 2018), whereas grey values are unacceptable.

A7 Comparison of soil isotopic composition within and beside former excavated material

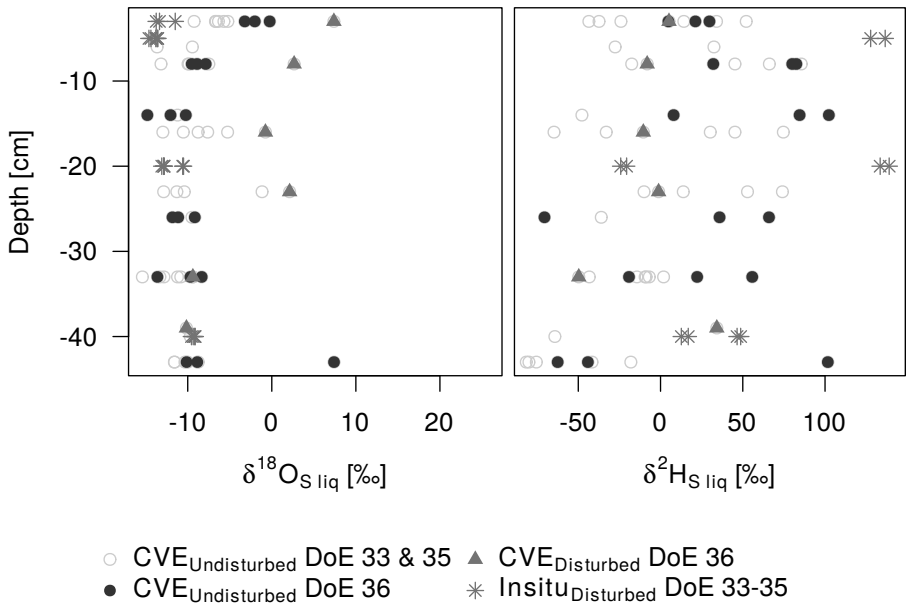

Figure A.5: Comparison of CVE soil isotopic composition sampled within sampled from the formerly excavated soil and samples from undisturbed soil. DoE 33-36 are displayed to account for spatiotemporal heterogeneities. *In situ* obtained values in the former disturbed area are also displayed.

A8 $\delta^{18}O$-$\delta^{2}H$ dual isotope space of transpiration isotope composition

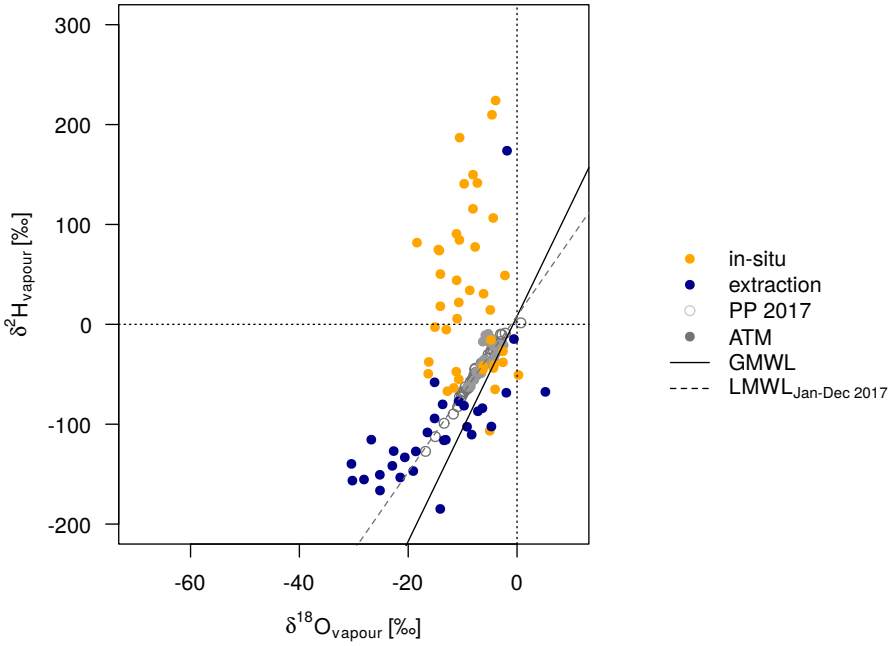

Figure A.6: Dual isotope plot of transpiration isotope composition. Values *in situ* are measured directly as vapour; whereas values from cryogenic vaccum extraction analysis are modeled from bulk leaf water analysis using the model from Craig and Gordon (Craig & Gordon 1965)

A9 Soil water potential

Soil water potential as soil physical characterization describing the (under)pressure necessary to extract water at a given volumetric soil water content contains important information about ability of plants to obtain water from a specific depth. Soil water potential at Freiburg Flugplatz experimental field site has been determined in the laboratory on soil cores (200 cm^3). Samples were taken in June 2018, in a distance of approximately 3 m from the experimental plot in the course of a bachelor's thesis submitted by Dahlmann (2018).

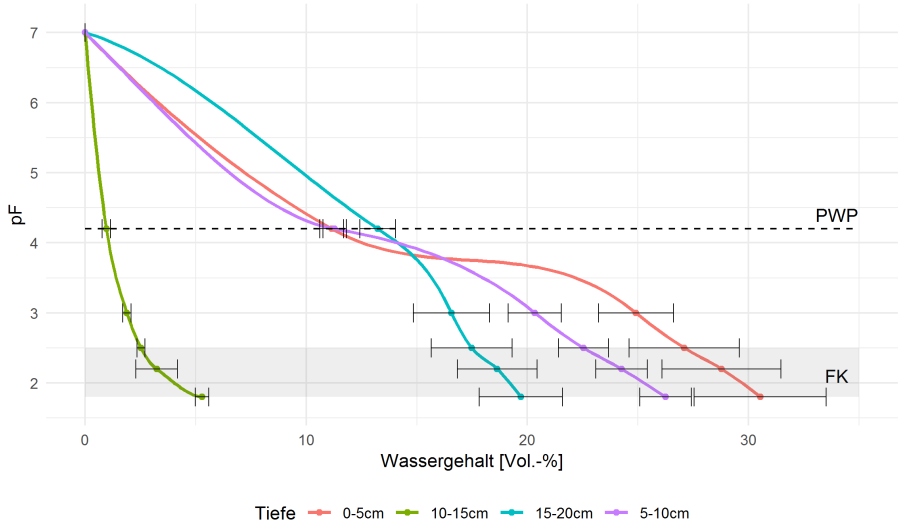

Figure A.7: Characteristic curves of mean soil water potentials at Freiburg Flugplatz experimental field site. Figure taken from Dahlmann (2018)

A10 In-situ measurement of photosynthesis and transpiration

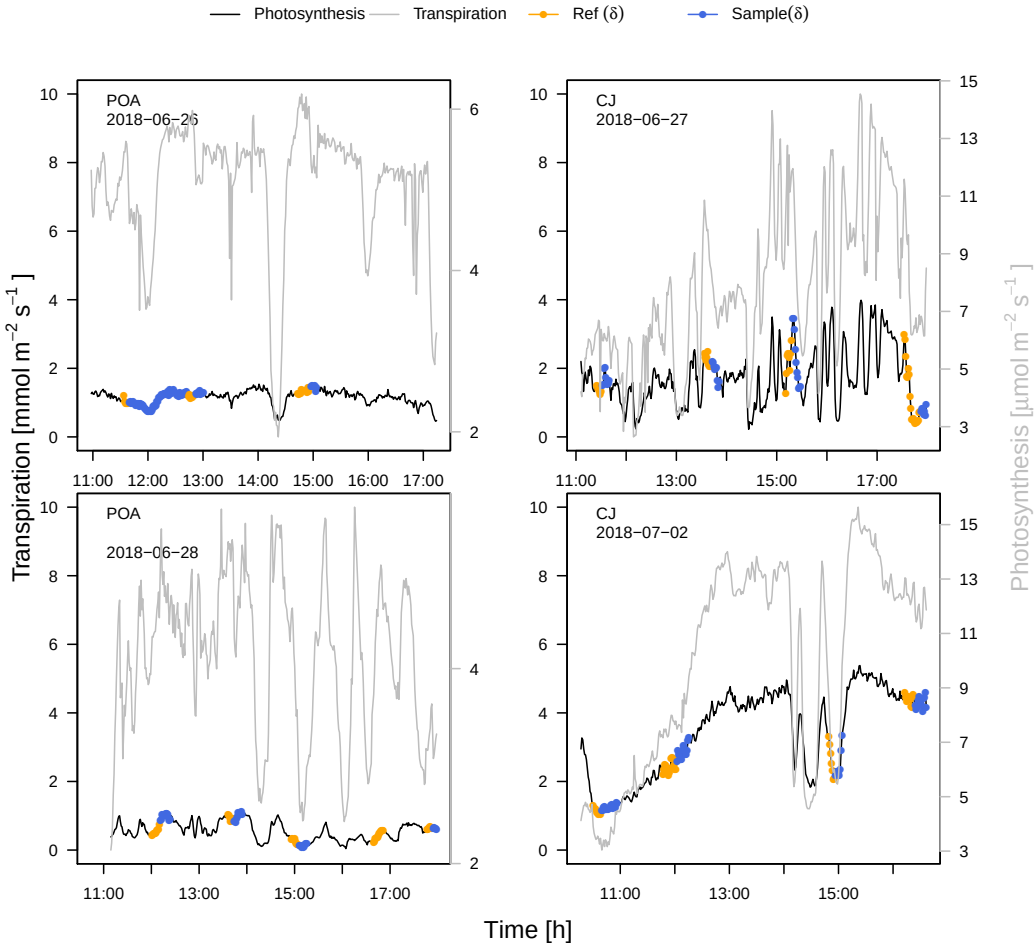

Figure A.8: Photosynthetic and transpiration rates of single leaf measurements *in situ* of *Centaurea jacea* (CJ) and *Arrhenatherum elatius* (POA). Each panel presents data over the course of four exemplary measurement days. Blue and orange coloured parts illustrate sequences, when the GFS system was coupled to the CRDS instrument. Measurement results are presented as calculated from the device default setting, with the measured leaf area assumed to be 4 cm^2. Values of *Arrhenatherum elatius* still need to be corrected for measured leaf area, which was usually smaller.